A thesis of the Degree of Doctor of Philosophy

Metabolic Regulation by Core Pluripotency Factors for Maintaining Embryonic Stem Cell Pluripotency

배아줄기세포의 전분화성 유지를 위한 Core Pluripotency Factor의 대사조절

August 2016

The Department of Biomedical Sciences
Seoul National University
Graduate School

Hyunsoo Kim

ABSTRACT

Pluripotent stem cells (PSCs) have distinct metabolic properties that support their metabolic and energetic needs and affect their stemness. In particular, high glycolysis is critical for the generation and maintenance of PSCs. However, it is unknown how PSCs maintain and acquire this metabolic signature. In this study, we found that core pluripotency factors regulate glycolysis directly by controlling the expression of glycolytic enzymes. Specifically, Oct4 directly governs Hk2 and Pkm2, which are important glycolytic enzymes that determine the rate of glycolytic flux. The overexpression of Hk2 and Pkm2 sustains high levels of glycolysis during embryonic stem cell (ESC) differentiation. Moreover, the maintenance of high glycolysis levels by Hk2 and Pkm2 overexpression hampers differentiation and preserves the pluripotency of ESCs in the absence of LIF. Overall, our study identifies a direct molecular connection between core pluripotency factors and ESC metabolic signatures and demonstrates the significance of metabolism in cell fate determination.

* This work is published in Stem Cells; published online September, 2015
DOI: 10.1002/stem.2073

Keywords: embryonic stem cells, core pluripotency factors, Oct4, metabolism, glycolysis, hexokinase 2 (Hk2), pyruvate kinase M2 (Pkm2), pluripotency, differentiation

Student number: 2009-30601

CONTENTS

LIST OF FIGURES AND TABLE

LIST OF ABBREVIATIONS

ESC	Embryonic stem cells
OSN	Oct4, Sox2, Nanog
Hk2	Hexokinase 2
Pkm2	Pyruvate kinase M2
OCR	Oxygen consumption rate
ECAR	Extracellular acidification rate
Dox	Doxycycline
Oct4 RE	Oct4 response element
AP	Alkaline phosphatase
EB	Embryoid body
RA	Retinoic acid
FACS	Flow cytometry
SCID	Severe combined immunodeficiency
DEGs	Differentially expressed genes

I. INTRODUCTION

Pluripotent stem cells (PSCs), including embryonic stem cells (ESCs) and induced PSCs (iPSCs), are promising tools for regenerative medicine and important resources for studying epigenetic and metabolic changes during the transition between cell hierarchies (Figure 1) (1-5). During such development, epigenetic alterations drive cell-type specific transcription of genes and metabolic changes without changes in genomic information. Metabolic shifts during cell hierarchical transitions are the result of adaptation mechanisms to meet growing metabolic and energetic needs and are actively involved in the regulation of epigenetics and transcription (6, 7).

Within the past decade, studies of metabolism in various stem cell populations have also highlighted a role for cell-specific metabolic pathways that are modulated during differentiation or during reprogramming to pluripotency. Before the morula stage of preimplantation embryos, each individual early blastomere is totipotent and retains the ability to generate an entire organism and its placenta (5). In totipotent stem cells, glycolysis is impaired due to the low activity of the rate-limiting enzymes hexokinase (Hk) and phosphofructokinase 1 (Pfk1). Therefore, for glucogenesis, these totipotent stem cells use pyruvate as their major energy and carbon source, to generate acetyl-CoA and oxaloacetate (OAA) via pyruvate dehydrogenase and pyruvate carboxylase (PC), respectively (8). Adenosine triphosphate (ATP) synthesis is dependent on mitochondrial oxidative phosphorylation driven by the electron transport chain (ETC) and ATP synthase. However, as mitochondrial replication does not occur at this stage, the halving of mitochondrial mass with each round of mitosis leads to a drop in ATP levels

during embryo cleavage (9, 10). Simultaneously, each mitochondrion matures and the inner mitochondrial membrane potential increases steadily, thereby converting the exponential drop in ATP into a linear drop. In this pathway, bicarbonate is needed as a pH buffer and to provide a carbon source for OAA generation in the Krebs cycle for anaplerosis via PC or for nucleotide synthesis for DNA and RNA via carbamoyl phosphate synthetase (11).

Metabolism of pluripotent stem cells and the blastocyst is different from that of the early embryo. During morula compaction, blastomeres undergo the first round of differentiation to segregate into the trophectoderm (which becomes the placenta) and the pluripotent inner cell mass (ICM, which becomes the embryo proper). Accompanying this transformation is a sharp increase in net growth and metabolic activity (5). Glucose flux increases with the increase in GLUT1/3 expression, and HK and PFK1 become activated to sharply increase glycolytic flux. As a result, flux into the pentose phosphate pathway (PPP) for nucleotide synthesis increases (12). ATP synthesis is more dependent on the reactions carried out by glycolytic phosphoglycerate kinases (PGKs) and pyruvate kinases (PKs), and is decoupled from O_2 consumption by the mitochondrial ETC (13). Activation of threonine dehydrogenase (TDH), glycine C-acetyltransferase (GCAT) and glycine decarboxylase (GLDC) promotes Thr-Gly catabolism to feed the folate one-carbon (1C) pool, which in turn fuels the synthesis of S-adenosylmethionine(SAM) and nucleotide to maintain pluripotency and proliferation (14).

When ESCs differentiate, the glycolytic flux decreases dramatically, Thr-Gly metabolism stops, and mitochondrial oxidative phosphorylation,

which is fueled by glucose and fatty acids, increases (14-17). Thus, cells acquire an even more oxidized state. Furthermore, pluripotent ESCs are enriched with unsaturated lipids such as omega 3 and omega 6 fatty acids, which contain readily oxidizable carbon-carbon double bonds. These unsaturated lipids prime ESCs for differentiation after oxidation by reactive oxygen species to form eicosanoids. This concept is supported by the finding that ESC pluripotency was preserved following pharmacological inhibition of enzymes in the eicosanoid synthesis pathway, which oxidize these unsaturated lipids (18).

The importance of metabolism in regulating stem cell biology is evident from studies that have shown the rapid and dynamic changes in substrate utilization during early embryogenesis (19). In the pre-implantation stage of mammalian development, cellular energy in the form of ATP is generated primarily through the oxidation of carbon sources such as lactate, pyruvate, amino acids, and fatty acids, which allow the generation of reducing equivalents that drive the ETC and oxidative phosphorylation (20-22). Additionally, the metabolite balance of both stem and differentiated cells has been found to directly influence the epigenome through post-translational modifications of histones, DNA, and transcriptional factors (23-28).

In general, metabolism is seen as a passive process that produces energy and building blocks to meet the demands of the specialized cells according to extra- or intra- cellular signals. However, recently, the active roles of metabolism have gained considerable research interest. Cells constantly adjust their metabolic state in response to extracellular signals and

nutrient availability. Conversely, the metabolic state of cells can affect signal transduction and cell hierarchy (7, 29-31).

The metabolic signatures of PSCs have recently been identified. One hallmark is that PSCs rely heavily on glycolysis compared with their differentiated counterparts. The expression of glycolysis-related genes and lactate production in human PSCs are higher than in differentiated cells (32-34). During the reprogramming of mouse and human somatic cells into iPSCs, lactate production rises, whereas oxygen consumption declines (Figure 2) (35, 36). High-glucose culture medium reprograms mouse somatic cells into iPSCs more efficiently than low-glucose medium (37, 38). A metabolomics analysis demonstrated that somatic cells convert from an oxidative state to a glycolytic state in pluripotency (39). Thus, these reports clearly show that high glycolysis is important for pluripotency, however, it is unknown how PSCs maintain and acquire high glycolysis levels or to what extent this metabolic signature affects pluripotency.

In this study, we postulated that core pluripotency factors regulate glycolytic enzymes directly to maintain and acquire high glycolysis levels. In earlier work on analyzing direct target genes of Oct4 in ESCs (37), we noted that Oct4 binds to the regions of several glycolytic enzyme genes. Preliminary experiments that examined changes in lactate production during Oct4 depletion strengthened our hypothesis. Additionally, it has been reported that the stemness factor Oct4 has a number of targets associated with energy metabolism, which may impact the balance between glycolysis (PC and Hk1) and oxidative metabolism (NDUFA3, ATP5D, and ATP5f1) (3). A

combination of chromatin immunoprecipitation-sequencing (ChIP-seq) and real-time quantitative PCR analysis of glycolytic enzymes, Oct4 directly regulated hexokinase 2 (Hk2) and pyruvate kinase M2 (Pkm2), the 2 most critical enzymes that govern glycolytic flux (37, 40-42).

Further, we found that overexpression of Hk2 and Pkm2 supports high glycolysis levels and impedes ESC differentiation. Hk2- and Pkm2-overexpressing ESCs retained pluripotency in the absence of the cytokine leukemia inhibitory factor (LIF). Our study demonstrates how ESC metabolic signatures are maintained at the molecular level and shows that metabolism fundamentally affects cell fate.

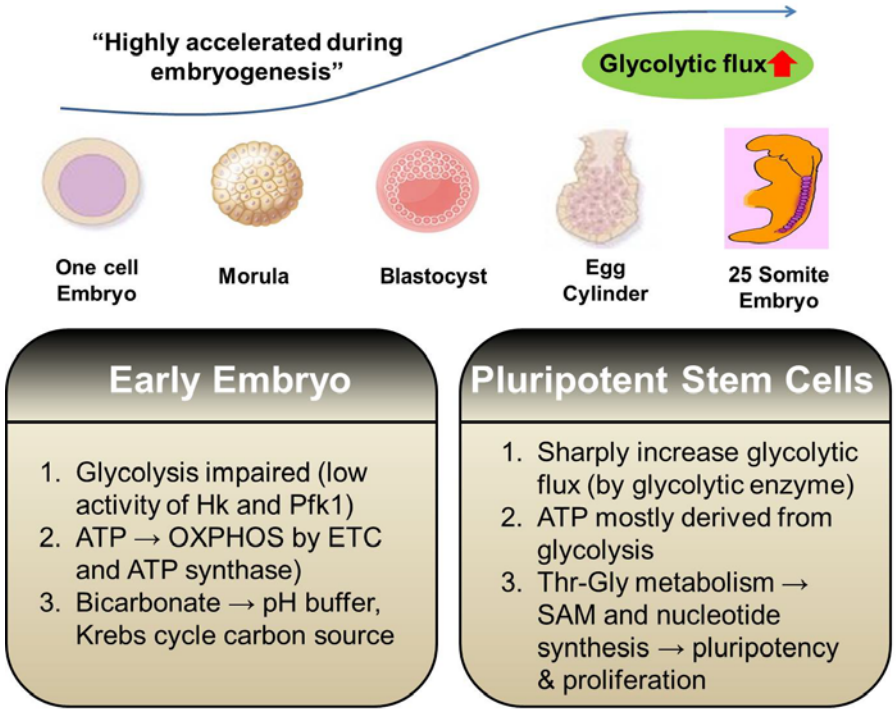

Figure 1. Metabolic dynamics during development.

Early embryos are initially depends upon oxidative metabolism. However, there is concomitant acceleration of anaerobic glycolysis during embryogenesis in pluripotent stem cells.

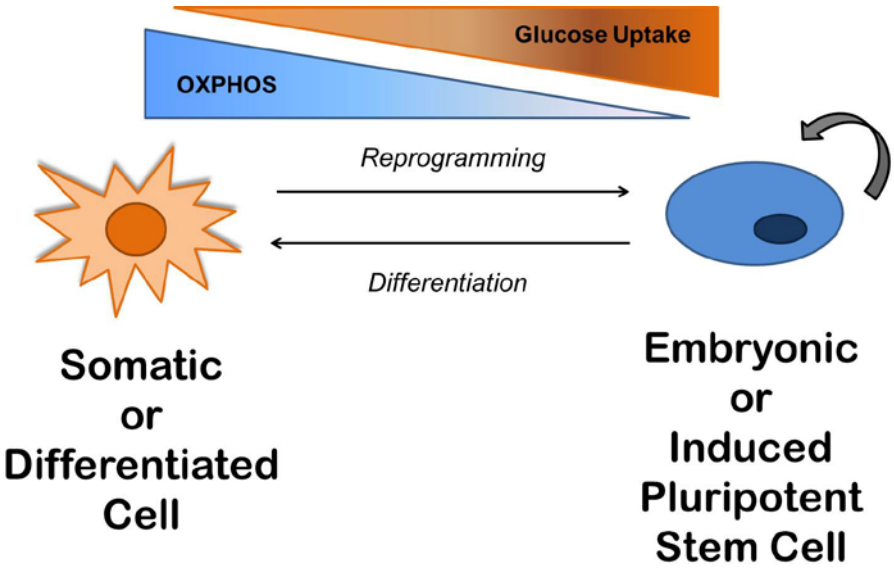

Figure 2. Glycolytic engagement stimulates pluripotent gene induction.

Glucose uptake is important in reprogramming efficiency during somatic cells convert from an oxidative state to a glycolytic state in pluripotency. OXPHOS, oxidative phosphorylation.

2. MATERIALS AND METHODS

1. Cell culture

Mouse ESCs were cultured by 2 methods. For a typical serum LIF culture, cells were cultured in a 0.1% gelatin (Sigma-Aldrich, St. Louis, MO, http://www.sigmaaldrich.com)-coated tissue culture dishes in the presence of LIF (1000 U/ml ESGRO ; Millipore, Darmstadt, Germany, http://www.merckmillipore.com) and 15% (v/v) fetal bovine serum (Gibco, Grand Island, NY, http://www.invitrogen.com) as described (37). For 2i cultures, N2B27 medium was prepared as described (43). ZHBTc4 cells were kindly provided by Hitoshi Niwa (RIKEN, Japan), and ZHBTc4 F-Oct4 cells have been described (37). Epiblast stem cells (EpiSCs) were cultured as described (44). All cells were cultured under normoxic conditions.

2. Transplantation assay

To evaluate the developmental effects of Hk2 and Pkm2 overexpression, cells were injected subcutaneously into severe combined immunodeficiency (SCID) mice (NOD.Cg-*Prkdc*^{scid} *Il2rg*^{tm1Wjl}/SzJ, Jackson Laboratory, Bar Harbor, Maine, http://www.jax.org) and maintained for 6–8 weeks. After 6–8 weeks, subcutaneous teratomas were dissected, fixed in 4% paraformaldehyde overnight, and stained with hematoxylin and eosin. Animal experimental procedures were approved by the Institutional Animal Care and Use Committee (IACUC) of Seoul National University, Korea (SNU-141128-2).

3. Generation of stable expression of Hk2 and Pkm2 in ESCs

For long-term transgenic expression in E14 and ZHBTc4 ESCs, human HK2 and PKM2 were cloned into pCAG-Flag-IRES-puromycin and pCAG-Flag-IRES-blasticidin, which were generated by modifying the pCAG-IP vector (45). To generate E14 ESCs overexpressing Flag-tagged HK2 and PKM2, both pCAG-Flag-HK2-IRES-blasticidin and pCAG-Flag-PKM2-IRES-puromycin were cotransfected into E14 cells using Lipofectamine (Invitrogen, Carlsbad, CA, http://www.invitrogen.com), and after 48 hr, E14 cells were doubly selected with puromycin (2 μg/ml) and blasticidin (2 μg/ml) for at least 2 weeks.

To generate ZHBTc4 ESCs overexpressing Flag-tagged HK2 and PKM2, both puromycin-resistant pCAG-Flag-IP HK2 and PKM2 were cotransfected into ZHBTc4 cells using Lipofectamine (Invitrogen), and puromycin selection (2 μg/ml) was performed for stable integration after 48 h. After 48 hr, individual surviving colonies were picked and used to seed 24-well plates. Until the cells grew properly, puromycin selection (2 μg/ml) was performed. Resistant cells were expanded and tested for HK2 and PKM2 expression by western blot.

4. Self-renewal assay

Self-renewal assay (colony-forming assay) was performed as described (37). Briefly, ESCs were trypsinized to single cell suspensions and replated at 500 cells per well in a 6-well plate. Doxycycline (Dox) was added 1 day after replating. After 3 days of incubation with or without Dox and LIF, the plates

were stained for alkaline phosphatase (AP) and scored for differentiation status and size.

5. *In vitro* differentiation of ESCs

ESCs were differentiated done as reported (37). Briefly, ESC differentiation was induced by LIF withdrawal from ESC medium, treatment with retinoic acid (RA) (0.5 uM) in LIF-depleted medium, and addition of serum-free N2B27 medium to monolayer cultures. For embryoid body (EB) formation, ESCs were cultured in low-attachment dishes that contained ESC medium without LIF. Oct4 depletion-mediated differentiation of ZHBTc4 cells was performed as described (46).

6. Reporter gene assay

To establish pHk2-luc and pPkm2-luc reporter constructs, which contained the promoter, first exon, and first intron of Hk2 and Pkm2, respectively, in which the first exon was replaced with the luciferase gene, PCR products from E14 genomic DNA were subcloned into pMSCV puro (Addgene, Cambridge, MA, http://www.addgene.org). Reporter gene activity was measured as described (37).

7. Western blot and immunofluorescence

Western blot and immunofluorescence were performed as described (37). Anti-Hk2 (2867) and anti-Pkm2 (4053) were purchased from Cell Signaling

Technology (Danvers, MA, http://www.cellsignal.com); anti-Nanog (ab14959) was purchased from Abcam (Cambridge, U.K., http://www.abcam.com); anti-Sox2 (MAB2018) antibody was obtained from R&D Systems (Minneapolis, MN, http://www.rndsystems.com); anti-Oct4 (sc-5279) was acquired from Santa Cruz Biotechnology (Dallas, Texas, http://www.scbt.com); anti-Pfkp (NBP1-19585) was purchased from Novus Biologicals (Littleton, CO, http://www.novusbio.com); and anti-Pdk1 (KAP-PK112) was obtained from Stressgen Bioreagents (San Diego, CA, http://www.stressgen.com). For immunofluorescent staining, cells on the cover glasses were fixed with 4% (w/v) paraformaldehyde, permeabilized with 0.5% (v/v) Triton X-100, and blocked with 2% (w/v) bovine serum albumin in phosphate-buffered saline. Endogenous or overexpressed proteins were immunostained with corresponding antibody and Rhodamine Red-X and FITC-conjugated secondary anti-mouse or rabbit IgG antibody (Jackson Immunoresearch). 50% (v/v) glycerol containing 4′,6-diamidino-2-phenylindole solutions are loaded on the slide glass and covered with cover glass. Immunofluorescence was observed under a Zeiss LSM 510 laser scanning microscope.

8. Real-Time qPCR and Chromatin immunoprecipitation (ChIP) assay

Preparation of RNA, reverse-transcription PCR, real-time qPCR, and chromatin immunoprecipitation (ChIP) were performed as described (37). For ChIP assay E14 and ZHBTc4 cells were harvested, cross-linked with formaldehyde to a final concentration of 1%. Cross-linking reaction was

stopped by adding glycine to a final concentration of 0.125M. Cells were harvested and washed twice with cold PBS and cytosolic fractions were eliminated with buffer A [5mM PIPES (pH 8.0), 85mM KCl, 0.5% NP-40, protease inhibitors]. Nuclear pellets were washed and resuspended in 1X Micrococcal nuclease reaction buffer [10mM Tris-Cl (pH 7.9), 5mM $CaCl_2$, 0.5mM DTT] and chromatin was digested with Micrococcal nuclease (New England Biolabs). Digestion reaction was stopped by addition of EDTA into the reaction buffer. Digested nuclear pellets were resuspended in buffer B [100mM Tris-Cl (pH 8.1), 1% SDS, 10mM EDTA, and protease inhibitors] and sonicated for disruption of nuclear membrane. Prepared chromatin fraction was diluted 1/10 in IP buffer (0.01% SDS, 1.1% TritonX-100, 1.2mM EDTA, 16.7mM Tris-Cl [pH 8.1), 167mM NaCl, and protease inhibitors] and incubated overnight at 4°C. Samples were incubated with salmon sperm DNA pre-coated protein A or G bead for 2~4 hours at 4°C, washed with TSE150 [0.1% SDS, 1% TritonX-100, 2mM EDTA, 20mM Tris-Cl (pH 8.1), 150mM NaCl], TSE500 [0.1% SDS, 1% TritonX-100, 2mM EDTA, 20mM Tris-Cl (pH 8.1), 500mM NaCl], BufferIII [0.25M LiCl, 1%NP40, 1% Sodium deoxycholate, 1mM EDTA, 10mM Tris-Cl (pH 8.1)], TE(pH 8.0) for two times. Washed beads were eluted with elution buffer (1% SDS, 0.1M $NaHCO_3$), incubated overnight at 65°C with NaCl for reversal of crosslinking. Samples were incubated 50°C in addition of 10μl of 0.5M EDTA, 20μl of 1M Tris (pH 6.5), and 4μl of Proteinase K (20mg/ml), purified with phenol/chloroform/isoamyl alcohol. Nucleic acid was precipitated by centrifugation 30 min at 4°C with 1μl glycogen solution (20mg/ml), 20μl

NaCl (5M), and 500ul isopropanol. Pellets were washed with 70% EtOH, dried and eluted with pure water. Sequences of the primers used for mRNA quantification and ChIP assay were described in Table 1.

9. Lactate assay

Lactate levels were measured using the Lactate Assay Kit (Biovision, Milpitas, CA, http://www.biovision.com) per the manufacturer's instructions. Pluripotent and differentiated cells were plated and cultured for 72 hr, at which point fresh medium was added to cells. After 3 hr, 200 $\mu\ell$ of medium was collected, and cells were counted. Lactate concentrations were normalized to cell number.

10. Extracellular flux analysis

Oxygen consumption rate (OCR) and extracellular acidification rate (ECAR) were determined on a Seahorse XF24 extracellular flux analyzer (Seahorse Bioscience, North Billerica, MA, http://www.seahorsebio.com) as described (47). Briefly, cells were cultured in 24-well cell culture microplates (Seahorse Bioscience) to ensure approximately 90% surface coverage at each time point. A Seahorse Bioscience instrument was used to measure the rate of change in dissolved O_2 and pH in the media. OCR and ECAR values were normalized to cell number.

11. Flow cytometry (FACS) analysis of SSEA1-positive cells

Cells were separated to single cells using trypsin/EDTA and incubated with Fc blocker to reduce nonspecific binding of antibodies. Cells were stained with anti-human/mouse SSEA-1 PE (eBioscience, San Diego, CA, http://www.ebioscience.com), and FACS analysis was performed at the Flow Cytometry Core (National Cancer Center) on a FACSVerse^{TM} flow cytometer (BD Biosciences, San Diego, CA, http://www.bdbiosciences.com).

12. Karyotype analysis

Mouse ESCs were karyotyped as described (48). Briefly, cells were harvested after 6 h of colcemid (100 ng/ml) treatment and incubated sequentially in a hypertonic solution (0.075M KCl) and a fixing solution (methanol/acetic acid, 3:1). The swollen cells were spread onto a glass slide and stained with 4',6-diamidino-2-phenylindole (DAPI; 100 ng/ml). Chromosome images were obtained from the Microscopy Core (National Cancer Center) on an LSM 510 META (Carl Zeiss, Jena, Germany, http://www.zeiss.com).

13. ChIP-sequencing

ChIP-sequencing was performed as described (37). ZHBTc4 F-Oct4 cells were ChIPed with anti-Flag. ChIPed DNA was sequenced by the KRIBB (Korean Research Institute of Bioscience & Biotechnology). Briefly, DNA fragments were ligated to a pair of adaptors for sequencing on an Illumina Hiseq-2000. The ligation products were size-fractioned to obtain 200–300-bp fragments on a 2% agarose gel and subjected to 18 cycles of PCR

amplification. Each library was diluted to 8 pM for 76 cycles of single-read sequencing on the Illumina Hiseq-2000 per the manufacturer's recommended protocol.

14. RNA-sequencing

Total RNA from E14 cells was extracted with QIAzol (QIAGEN, KJ Venlo, Netherlands, http://www.qiagen.com) and sequenced by Macrogen (Seoul, Korea, http://dna.macrogen.com) on a Hiseq-2000 (Illumina).

15. RNA-sequencing data analysis

Reads for each sample were aligned to the mouse genome (NCBI build 37/mm9) using TopHat v2.0.7 (49) with default settings. Cufflinks v2.0.2 (50) was used to quantify FPKM values of genes, defined from RefSeq transcripts. A normalized gene expression table was collected using DESeq v1.16.0 (51). Unsupervised hierarchical clustering analysis of gene expression was performed using Cluster 3.0, and the results were visualized with Java TreeView. Differentially expressed genes (DEGs) were defined by applying edgeR v2.12 (52), with an FDR < 0.05. For defined DEGs, gene ontology analysis was conducted using DAVID (53). Other statistical tests were performed using R statistical packages.

16. Accession numbers

The ChIP-seq and RNA-seq datasets have been deposited into the NCBI Gene Expression Omnibus (GEO) database under accession numbers GSE36388 and GSE65246.

17. Statistics

Statistical analysis was done as reported (54). Briefly, data were presented as means ± standard deviations, and P values were calculated using the student's t-test calculator. All data were representative of at least 3 separate experiments.

	Gene	5’ primer	3’ primer
Real-time PCR	*Hk1*	CACCGGCAGATTGAGGAAAC	CTCAGCCCCATTTCCATCTCT
	Hk2	AGCTGCTGTTCCAAGGGAAACTCA	GTAGGCCTTCTGAATTCCGTCCTT
	Hk3	TCTTCCGAGGCCAGAAGACTCAAT	AGGCGTCATCAGATGTCAGAGTCA
	Gck (*Hk4*)	GGGTCATAAATCGCATGCGCGAAA	AAGGTGATTTCGCAGTTGGGTGTC
	Pfkm	GTGTGGAAGCAGTGATGGCACTTT	TAGCCTTGGTCACGTCTTTGGTCA
	Pfkl	GAGAAGATGAAGACAGACATCC	CCAGTTTGGTCCCATAGTTC
	Pfkp	CTGCCAAAGCAATGGAGTGGATCT	CAGTGACTTTCTTCAGCTCTGCCA
	Pkm	TGGGAGAGAAGGGCAAGAACATCA	TCTCTGCAGGAATCTCAATGCCCA
	Pklr	CTGCTGTCATTGCTGTGACTCGTT	AAGCCACGAAGCTTTCCACTTTCG
	Pkm2	ACTTGCAGCTATTCGAGGAACTCCG	GGGATTTCGAGTCACGGCAATGAT
	Pkm1	TCTGCTGTTTGAAGAGCTTGTGCG	GGGATTTCGAGTCACGGCAATGAT
	Gpi1	AAGTCCAGAGGCGTGGAGGC	ACCCTGTTCACCTCCGGCAT
	Tpi1	AGCACCCGGATCATTTATGGAGGT	GGGCAGTGCTCATTGTTTGGCATT
	Aldoa	ATGCTTGCACCCAGAAAT	CGACCATAGGAGAAAGTCAAG
	Aldob	TCCTCTTTAGTGTGGACAATTC	GAATGGTGGTTTCCTTGTTTG
	Aldoc	GAACGCTGTGCTCAGTATAA	GAACGCTGTGCTCAGTATAA
	Pgk1	CAAGGCTGCTGTTCCAAGCATCAA	TGAGTTCAGCAGCAACTGGCTCTA
	Pgk2	CCCTATGCCAGACAAGTATTC	CTTTACCCTTACCTTCTTCCTC
	Pgam1	GATGCCATTGACCAGATGT	TGCTGATGTTGCTGTAGAAG
	Pgam2	TGGATGTTACGGACCAAATG	GGAGGTGTAGTAGTTGTGTT

			TC
	Pdk1	CCGGGCCAGGTGGACTTC	GCAACTCTTGTCGCAGAAAC ATAAA
	Pdk2	TACAAGGACACCTATGGAGA T	TCTTTCACCACATCAGACAC
	Pdk3	CCTTGGCTGGATTTGGTTAT	CTTCAGGAGTGGTCTTGTAA TG
	Pdk4	ATGTCAGGTTATGGGACAGA CGCT	TTCTTCGGTTCCCTGCTTGG GATA
	Eno1	TGAGGGTGGATTCGCACCTA ACAT	CAGCCACATCCATGCCAATG ACAA
	Eno2	GGGTCATCAAGGACAAGTAT G	TCCAAGTCGTATTTGCCATC
	Eno3	GCCTGTAAACTTGCACAATC	TCCTCATAAGCTGGTTGTAT TT
	Ldha	CTGAAGTCTCTTAACCCAGA AC	ATCATGGTGGAAATGGGATG
	Ldhb	TGACCTCATCGAGTCCATGC TGAA	CAGCTTCTGATTGATGACGC TGGT
	Ldhc	TGTATCTGCCAACTCCAAAC	TATCTTCCAAACCACGTATG TC
	Gapdh	CCCACTAACATCAAATGGGG	CCTTCCACAATGCCAAAGTT
	Gapdhs	CAGTGCAAAGACCCTAAAGA	GGTTATAGTCCTTCTCGTTC AC
	18s rRNA (control)	TTAGAGTGTTCAAAGCAGGC CCGA	TCTTGGCAAATGCTTTCGCT CTGG
	Actb(control)	ATCACTATTGGCAACGAGCG	TCAGCAATGCCTGGGTACAT
ChIP	*Hk2 Pro*	TCTCGGCGCGCCATTTACAT AAGA	AATCCTGGACTAGGGTAGG AACCA
	Pkm2 Pro	CATCCTTTCAACCTCCATATC C	AATAGCGGCCAACCTTTC
	Nanog Pro	TTAGATCAGAGGATGCCCCC TAAG	CTCCTACCCTACCCACCCCC TATT

Table 1. Primers used in Results

3. RESULTS

1. Core pluripotency factors regulate a subset of glycolytic enzymes

To determine whether core pluripotency factors regulate ESC metabolism, we first measured alterations in metabolic flux on changes in core pluripotency factor protein levels. Doxycycline (Dox)-dependent depletion of Oct4 in ZHBTc4 cells (46) resulted in a rapid decrease in Oct4, Sox2, and Nanog (OSN), and recovery of Oct4 protein restored OSN protein levels (Figure 3). In this system, we examined lactate production and extracellular acidification (ECAR) rates as markers of glycolytic flux and oxygen consumption rate (OCR) as a marker of oxidative phosphorylation flux (4). Lactate production rate (Figure 4A) and ECAR (Figure 4B) were proportional to OSN levels, whereas OCR (Figure 4C) was inversely proportional to them, suggesting that OSN upregulates glycolysis.

Then, we examined the possibility that core pluripotency factors directly regulate glycolytic enzymes. To this end, we determined whether core pluripotency factors occupied the regions of glycolytic enzyme genes using chromatin immunoprecipitation-sequencing (ChIP-seq) data from our study and 3 other reports (40-42). Based on our screen of OSN occupancy in these regions, including those of isoforms (Figure 5), core pluripotency factors co-occupied many regions of glycolytic enzyme genes (Figure 6 and 7). These data suggest that core pluripotency factors regulate metabolic flux via direct regulation of glycolytic enzymes.

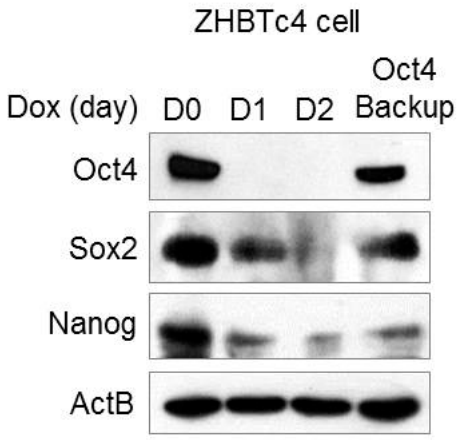

Figure 3. Core pluripotency factors expression depends on Oct4.

Whole cell lysates from ZHBTc4 cells and ZHBTc4 F-Oct4 cells on addition of Dox were analyzed by Western blot. Sox2 and Nanog expression levels were changed depends on Oct4 expression. ActB was used as a loading control.

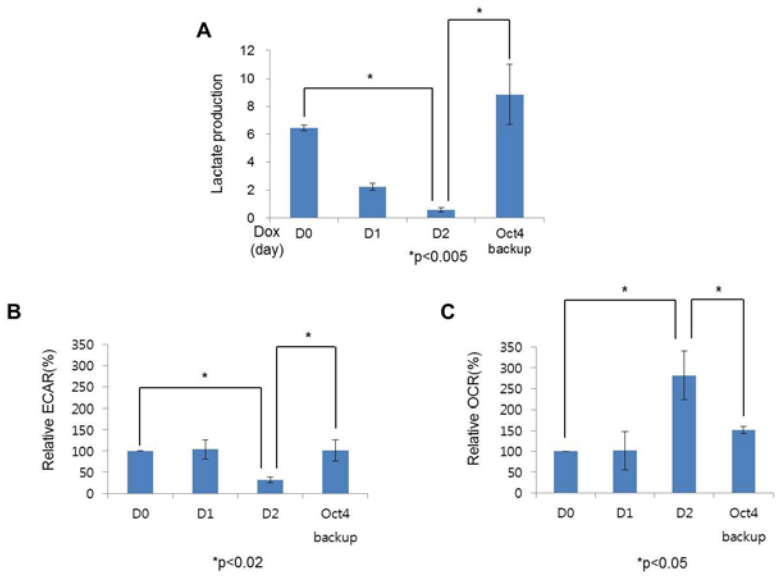

Figure 4. Core pluripotency factors target a subset of glycolytic enzymes.

(**A-C**) Changes in lactate production rates, ECAR, and OCR were determined in ZHBTc4 and ZHBTc4 F-Oct4 cells on addition of Dox. The lactate production and extracellular acidification (ECAR) rates as markers of glycolytic flux and oxygen consumption rate (OCR) as a marker of oxidative phosphorylation. Lactate production and ECAR levels were changed depends on Oct4, Sox2, and Nanog level. Inversely, OCR level was increased when lactation production decreased. Values represent mean ± standard deviation ($n \geq 3$).

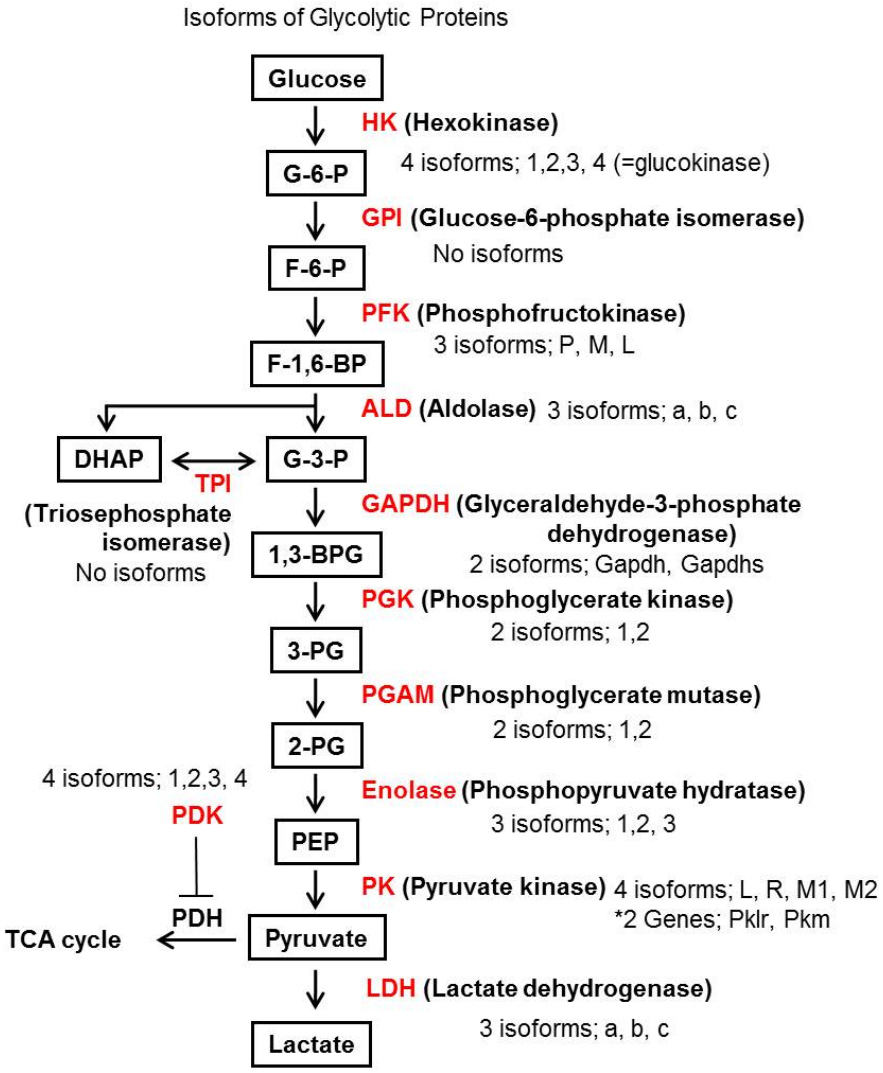

Figure 5. Putative Oct4, Sox2, and Nanog (OSN) target genes.

Isoforms of glycolytic enzymes.

Gene	Oct4 ChIP-Seq			Sox2 ChIP-Seq	Nanog ChIP-Seq
	Jang et al.	Ang et al.	Marson et al.	Whyte et al.	
Hk1	target	target	-	-	-
Hk2	target	target	target	target	target
Hk3	-	target	target	-	-
Gck (Hk4)	target	target	target	target	-
Gpi1	target	target	target	target	-
Pfkm	target	-	target	target	target
Pfkl	-	-	target	target	-
Pfkp	target	target	target	target	target
Aldoa	-	-	-	target	target
Aldob	-	-	-	-	-
Aldoc	target	-	-	-	-
Tpi1	target	-	target	target	target
Gapdh	target	target	target	target	-
Gapdhs	target	-	-	-	-
Pgk1	target	target	-	target	-
Pgk2	-	-	-	-	-
Pgam1	-	target	-	-	target
Pgam2	target	-	-	target	target
Eno1	target	target	target	-	-
Eno2	-	target	-	target	target
Eno3	-	-	-	-	target
Pklr	target	target	-	target	target
Pkm1	-	-	-	target	target
Pkm2	target	target	-	target	target
Ldha	-	-	-	-	-
Ldhb	-	target	target	target	-
Ldhc	-	-	-	-	-
Pdk1	target	target	target	target	target
Pdk2	-	-	-	-	target
Pdk3	-	-	-	-	target
Pdk4	target	target	-	-	target

Figure 6. ChIP-sequencing analysis of Oct4, Sox2, and Nanog (OSN) target genes.

Putative OSN target genes. Using our findings and public chromatin immunoprecipitation sequencing (ChIP-seq) data, OSN occupancy in the gene regions of entire glycolytic enzymes was examined. According to ChIP-seq data, OSN co-occupied many of glycolytic gene regions.

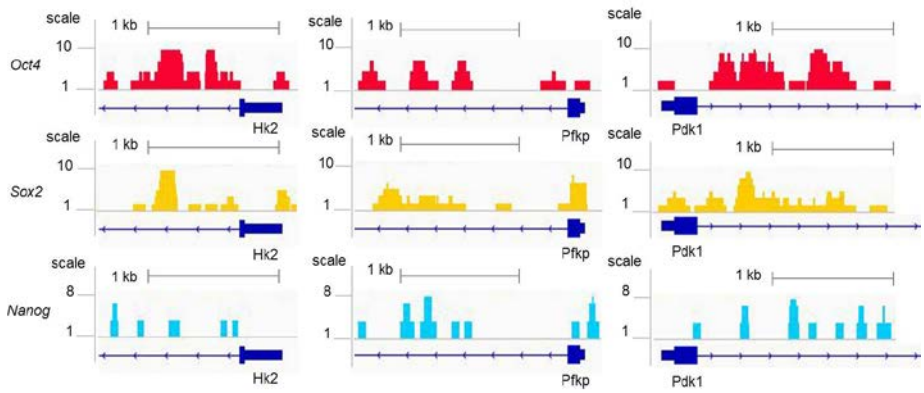

Figure 7. ChIP-seq binding profiles for potential OSN target genes.

Based on ChIP-seq data from our study and three other reports, Hk2, Pfkp, and Pdk1 has been identified as common glycolytic genes occupied by OSN.

Thus, we screened the glycolytic enzymes that were transcriptionally regulated by core pluripotency factors by measuring changes in their mRNA levels using 3 systems. First, we used ZHBTc4 and ZHBTc4-F-Oct4 cells, in which we reported that Oct4 transcriptional activity is proportional to its protein level (37) in typical serum LIF culture conditions. Then, we used ZHBTc4 and ZHBTc4-F-Oct4 cells in 2-inhibitor (2i) culture conditions (55). Lastly, we performed E14 cell differentiation into embryoid bodies (EBs) in serum LIF conditions, because we have reported that Oct4 transcriptional activity declines rapidly during EB formation (37).

In these systems, the levels of 4 enzymes (Hk2, Pfkp, Pkm2, and Pdk1) changed consistently in proportion to Oct4 transcriptional activity (Figure 8 and 9). We then tested whether the mRNA levels of these enzymes reflected their protein levels. Notably, the protein levels of only 2 enzymes (Hk2 and Pkm2) were proportional to their mRNA amounts (Figure 10).

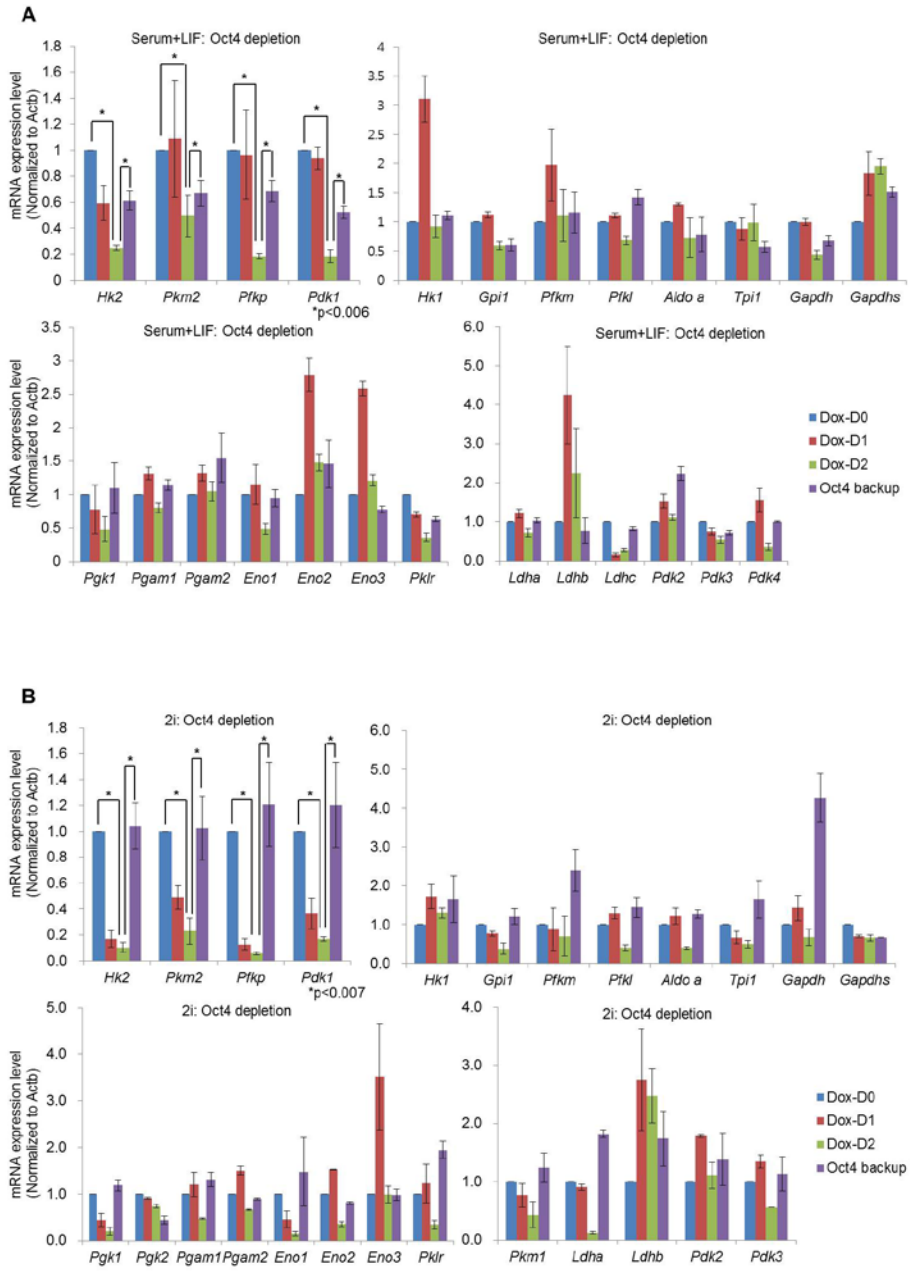
A
Serum+LIF: Oct4 depletion
mRNA expression level (Normalized to Actb)
Hk2
Pkm2
Pfkp
Pdk1
*p<0.006
Serum+LIF: Oct4 depletion
Hk1
Gpi1
Pfkm
Pfkl
Aldo a
Tpi1
Gapdh
Gapdhs
Serum+LIF: Oct4 depletion
mRNA expression level (Normalized to Actb)
Pgk1
Pgam1
Pgam2
Eno1
Eno2
Eno3
Pklr
Serum+LIF: Oct4 depletion
Ldha
Ldhb
Ldhc
Pdk2
Pdk3
Pdk4
Dox-D0
Dox-D1
Dox-D2
Oct4 backup
B
2i: Oct4 depletion
mRNA expression level (Normalized to Actb)
Hk2
Pkm2
Pfkp
Pdk1
*p<0.007
2i: Oct4 depletion
Hk1
Gpi1
Pfkm
Pfkl
Aldo a
Tpi1
Gapdh
Gapdhs
2i: Oct4 depletion
mRNA expression level (Normalized to Actb)
Pgk1
Pgk2
Pgam1
Pgam2
Eno1
Eno2
Eno3
Pklr
2i: Oct4 depletion
Pkm1
Ldha
Ldhb
Pdk2
Pdk3
Dox-D0
Dox-D1
Dox-D2
Oct4 backup

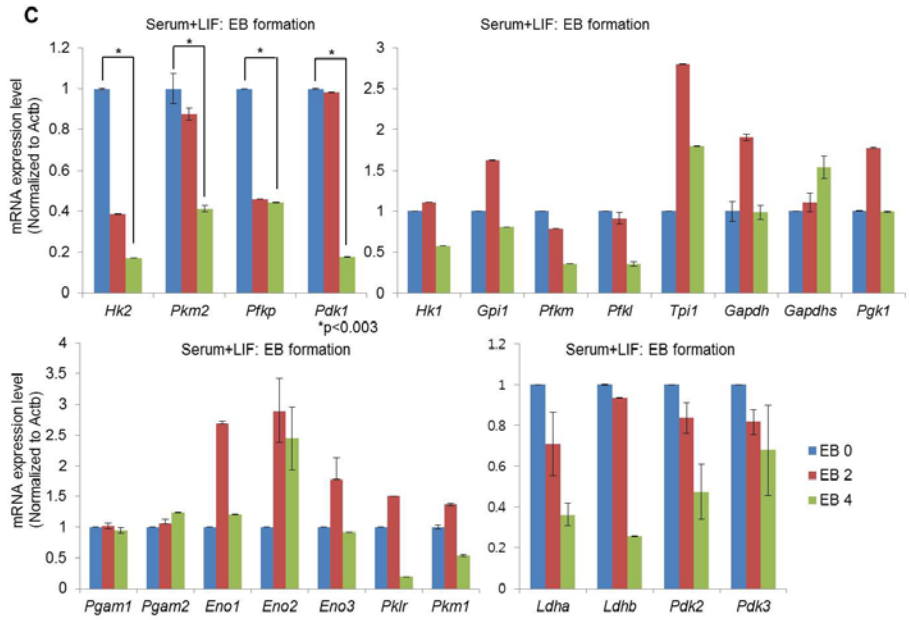

Figure 8. Screen of putative Oct4 target glycolytic enzymes in 3 systems.

Screen of putative Oct4 target glycolytic enzymes in 3 systems. ZHBTc4 cells, cultured in serum plus LIF medium (Serum+LIF) (**A**) or 2 inhibitors (2i) (**B**), were treated with Dox to deplete Oct4. Additionally E14 cells were differentiated into embryoid bodies (EBs) (**C**). Then, mRNA levels of entire glycolytic enzymes were analyzed by real-time qPCR. Relative mRNA expression levels are expressed as mean ± standard deviation (n≥3).

Gene	Serum+LIF (Oct4 depletion)	2i (Oct4 depletion)	Serum+LIF (EB formation)
Hk1	X	X	X
Hk2	O	O	O
Hk3	-	-	-
Gck (Hk4)	-	-	-
Gpi1	X	O	X
Pfkm	X	X	O
Pfkl	O	X	O
Pfkp	O	O	O
Aldoa	X	X	-
Aldob	-	-	-
Aldoc	-	-	-
Tpi1	X	O	X
Gapdh	O	X	X
Gapdhs	X	X	X
Pgk1	O	O	X
Pgk2	-	-	-
Pgam1	X	O	X
Pgam2	X	X	X
Eno1	O	O	X
Eno2	X	X	X
Eno3	X	X	X
Pklr	O	O	X
Pkm1	-	O	X
Pkm2	O	O	O
Ldha	X	O	O
Ldhb	X	X	O
Ldhc	O	-	-
Pdk1	O	O	O
Pdk2	X	X	O
Pdk3	X	X	X
Pdk4	O	-	-

Figure 9. Four glycolytic enzymes were putative Oct4 target genes.

Four enzymes—Hk2, Pfkp, Pkm2, and Pdk1—were putative Oct4 target genes the 3 systems. The mRNA levels of four enzymes changed depends on Oct4 level.

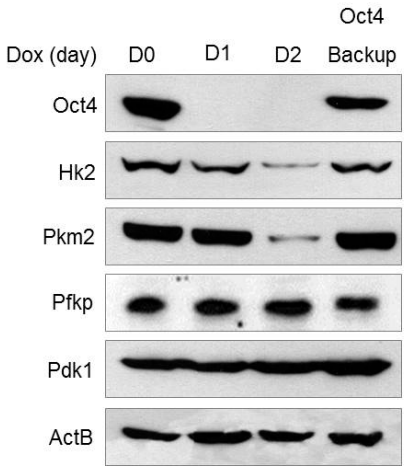

Figure 10. Protein expression levels of 4 putative Oct4 target genes.

Protein levels of 4 putative Oct4 target genes were assessed by western blot in ZHBTc4 cells. Only two enzymes (Hk2 and Pkm2) mRNA and protein levels were proportional to Oct4 level. ActB was used as a loading control.

2. Oct4 directly regulates Hk2 and Pkm2 in embryonic stem cells

To determine whether core pluripotency factors directly regulate the transcription of Hk2 and Pkm2, we analyzed the genome-wide occupancy of OSN in the Hk2 and Pkm2 genes. Based on integrative genomic viewer (IGV) data (42, 56), OSN occupied both the Hk2 and Pkm2 genes (Figure 11A). In these areas, we identified well-conserved Oct4 response elements (Oct4 REs), particularly in the first intron of both Hk2 and Pkm2 (Figure 11B).

To confirm the ChIP-seq data, we performed conventional ChIP assay in E14 and ZHBTc4 cells and analyzed Oct4 occupancy in the Oct4 REs of Hk2 and Pkm2. Oct4 occupancy of the Oct4 RE of the Nanog promoter was used as a positive control (37). Oct4 occupancy in the Hk2 gene was comparable with that of the Nanog gene (Figure 12A). Oct4 significantly bound the Pkm2 gene, although to a lesser extent versus the Nanog gene (Figure 12A).

Next, we tested whether this binding translated into gene transcription. We constructed a reporter gene that spanned the promoter, first exon, and first intron of Hk2 and Pkm2, in which the first exon was replaced with the luciferase gene. After stably incorporating these reporter genes into the genome of ZHBTc4 cells, we measured luciferase activity during Oct4 depletion.

Oct4 depletion significantly decreased luciferase activity time-dependently of the Hk2 and Pkm2 reporter genes (Figure 12B). We also stably incorporated these reporter genes into NIH3T3 cells, which do not express Oct4 (37). The addition of Oct4 significantly increased the luciferase activity of both

reporters (Figure 12C). These data demonstrate that Oct4 directly regulates the transcription of Hk2 and Pkm2 in ESCs.

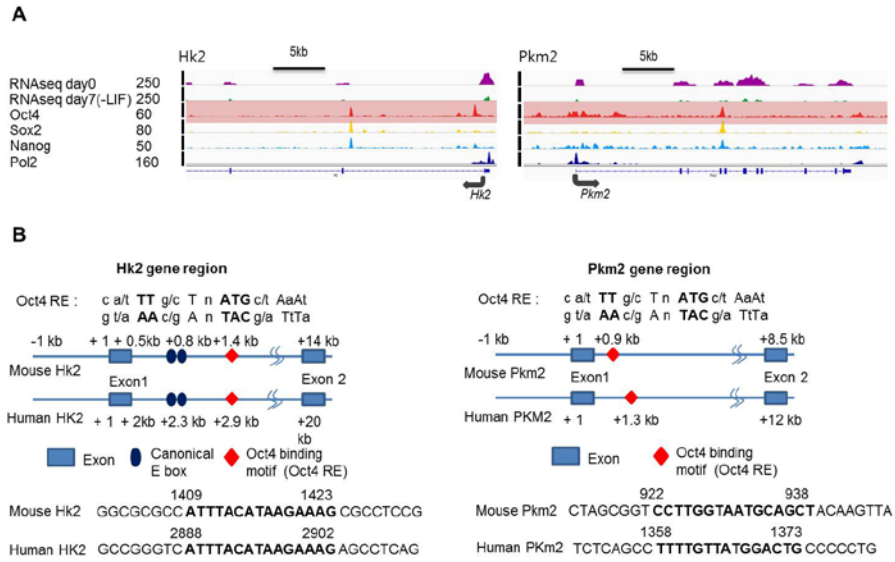

Figure 11. Gene region analysis of the Hk2 and Pkm2 genes.

(**A**) Integrated genomics viewer (IGV) showing OSN enrichment in the Hk2 and Pkm2 genes. OSN both occupied in the Hk2 and Pkm2 genes. (**B**) Schematic of well-conserved Oct4 response elements (Oct4 REs) in the Hk2 and Pkm2 genes.

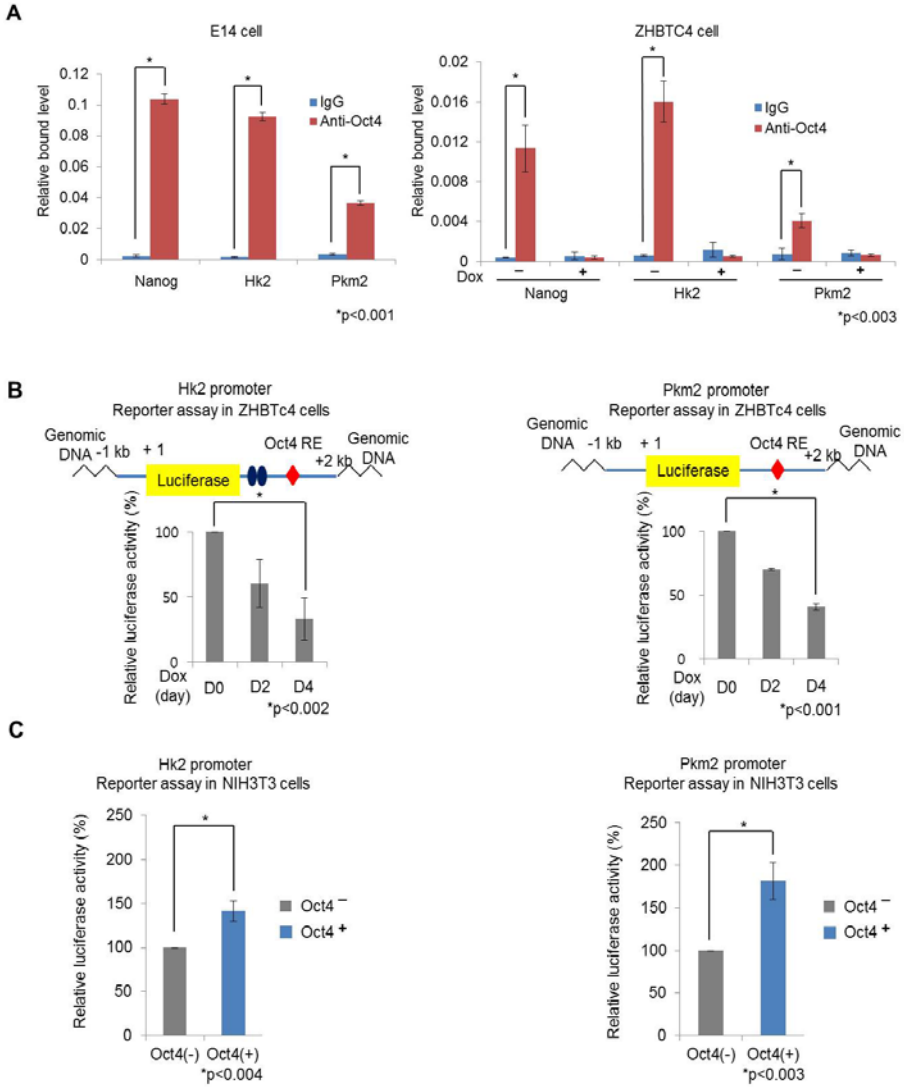
A
E14 cell
Relative bound level
0.12
0.1
0.08
0.06
0.04
0.02
0
IgG
Anti-Oct4
Nanog
Hk2
Pkm2
*p<0.001
ZHBTC4 cell
0.02
0.016
0.012
0.008
0.004
0
Dox
–
+
*p<0.003
B
Hk2 promoter
Reporter assay in ZHBTc4 cells
Genomic DNA
-1 kb
+ 1
Luciferase
Oct4 RE
+2 kb
Genomic DNA
Relative luciferase activity (%)
100
50
0
Dox (day)
D0
D2
D4
*p<0.002
Pkm2 promoter
Reporter assay in ZHBTc4 cells
*p<0.001
C
Hk2 promoter
Reporter assay in NIH3T3 cells
250
200
150
100
50
0
Oct4 –
Oct4 +
Oct4(-)
Oct4(+)
*p<0.004
Pkm2 promoter
Reporter assay in NIH3T3 cells
*p<0.003

Figure 12. ChIP and repoter gene analysis of Hk2 and Pkm2 gene regions.

(**A**) ChIP-qPCR analyses of Oct4 binding at the Oct4 RE in the Hk2 and Pkm2 genes. Nanog promoter was used as a positive control. Oct4 strongly binds to Oct4 binding regions of both Hk2 and Pkm2 genes. Values represent mean ± standard deviation (n≥3). (**B**) Reporter genes spanning the promoter, first exon, and first intron of Hk2 and Pkm2, in which the first exon is replaced with the luciferase gene (named pHk2–Luc and pPkm2–Luc), were stably incorporated to ZHBTc4 cells. Cells were treated with Dox. Luciferase activity was measured at the indicated time points with a luminometer. The luciferase activity decreases rapidly during Oct4 depletion. The values are expressed as relative percent mean luminescent units ± standard deviation (n≥3). (**C**) pHk2–luc and pPkm2–luc reporter genes were stably incorporated into the genome of NIH 3T3 cells. These stable cells, which have no endogenous Oct4, were infected with retroviral Oct4. The activity of both reporters increased in the addition of Oct4. Luciferase activity was measured 2 days after infection (n≥3).

3. Sustaining high levels of glycolysis delays ESC differentiation

Next, we examined whether overexpression of Hk2 and Pkm2 could maintain glycolysis in the absence of Oct4. Hk2 and Pkm2 were overexpressed in ZHBTc4 cells (ZHBTc4 Flag-Hk2&Pkm2). The addition of Dox reduced OSN and endogenous Hk2 and Pkm2 level, but ZHBTc4 Flag-Hk2&Pkm2 cells continued to express exogenous Hk2 and Pkm2 (Figure 13). Dox gradually reduced the lactate production rate and ECAR in control cells (ZHBTc4 Flag-Mock) but not in ZHBTc4 Flag-Hk2&Pkm2 cells (Figure 14A and 14B). Conversely, DOX upregulated OCR in control cells but not in Hk2- and Pkm2-overexpressingg cells (Figure 14C). These data suggest that the overexpression of both Hk2 and Pkm2 maintains glycolysis levels in the absence of Oct4.

Notably, ZHBTc4 Flag-Hk2&Pkm2 cells were more resistant to differentiation on depletion of Oct4. After 2-day treatment with Dox, ZHBTc4 Flag-Mock cells were nearly completely differentiated, whereas ZHBTc4 Flag-Hk2&Pkm2 cultures harbored a significant number of undifferentiated colonies (Figure 15). To determine the impact of alterations in metabolism on ESC pluripotency, we performed an experiment to compare tendencies with regard to ESC differentiation. Typically, the withdrawal of LIF sufficiently drives all E14 ESC populations to differentiate completely, but re-addition of LIF cannot restore these ESCs to the pluripotent state. However, if we withdraw LIF for the short term (cultured without LIF up to 24h), certain ESC populations fail to cross the threshold between differentiation and pluripotency, for which the re-addition of LIF at this time point (cultured

without LIF up to 24h) restores pluripotency.

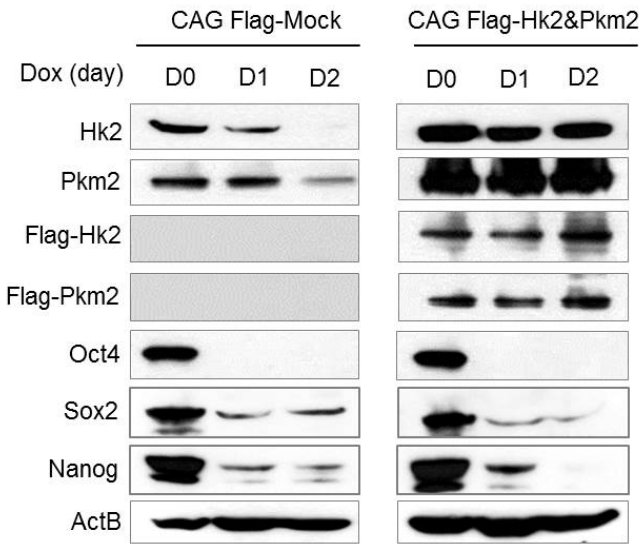

Figure 13. Protein expression levels of Hk2 and Pkm2 overexpression cells.

Flag-tagged human Hk2 and Pkm2 were stably transfected into ZHBTc4 cells. The levels of Hk2 and Pkm2 during Dox treatment were determined by Western blot. Expression of OSN were significantly decreased during Dox treatment, however, levels of Hk2 and Pkm2 were maintained in the overexpression cell. ActB was used as a control.

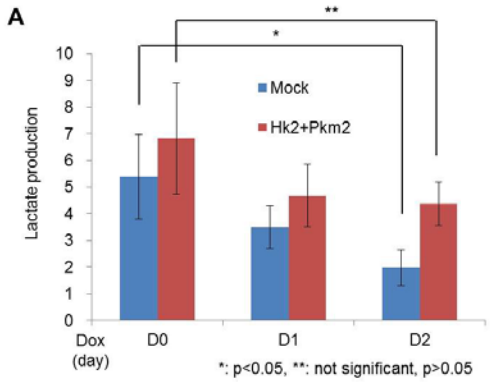
A
**
*
Lactate production
10
9
8
7
6
5
4
3
2
1
0
Mock
Hk2+Pkm2
Dox
(day)
D0
D1
D2
*: p<0.05, **: not significant, p>0.05

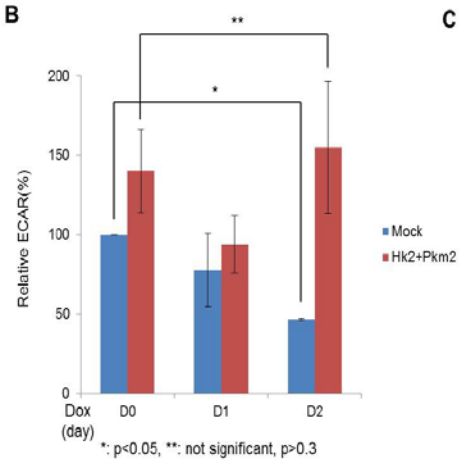
B
**
*
Relative ECAR(%)
200
150
100
50
0
Mock
Hk2+Pkm2
Dox
(day)
D0
D1
D2
*: p<0.05, **: not significant, p>0.3

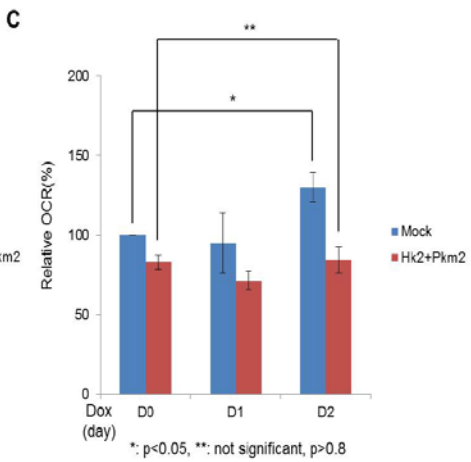
C
**
*
Relative OCR(%)
200
150
100
50
0
Mock
Hk2+Pkm2
Dox
(day)
D0
D1
D2
*: p<0.05, **: not significant, p>0.8

Figure 14. Overexpression of Hk2 and Pkm2 sustains high glycolytic flux during ESC differentiation.

(**A-C**) During Oct4 depletion, control cells lost lactate production and ECAR rates, whereas Hk2- and Pkm2-overexpressing cells retain higher lactate production and ECAR rates. The OCR rates increased in wild-type cells while no differences in overexpressing cells. Values represent mean ± standard deviation ($n \geq 3$).

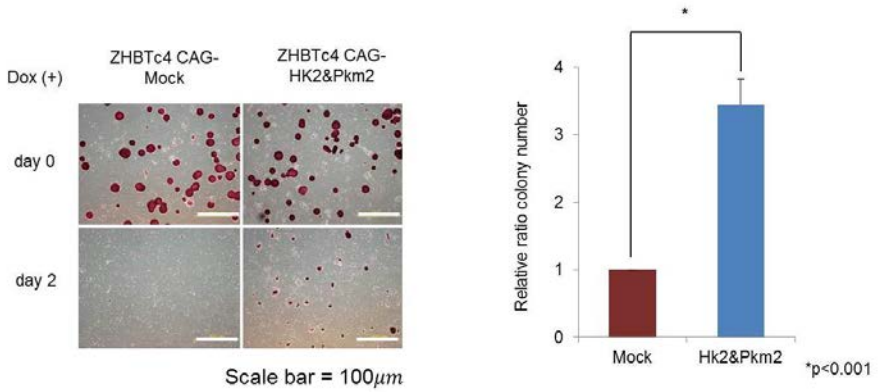

Figure 15. ZHBTc4 ESCs differentiation is delayed on depletion of Oct4 by overexpression of Hk2 and Pkm2.

After 2-day treatment with Dox, ZHBTc4 Flag-Mock and ZHBTc4 Flag-Hk2&Pkm2 cells were stained with AP and the numbers of AP-positive cells were counted. In overexpression cells, many of AP positive cells were maintained relative to control cells. Values represent mean ± standard deviation (n≥3).

The withdrawal of LIF for 12 h was insufficient to drive ESCs to differentiate, and re-addition of LIF nearly completely restored ESC pluripotency. In contrast, 48 h was sufficient to drive ESCs to differentiate, and re-addition of LIF failed to restore any pluripotent cells (Figure 16). Withdrawal of LIF for 24 h drove ~60% of cells to cross the differentiation threshold, whereas overexpression of Hk2 and Pkm2 impeded this differentiation—~20% of cells passed the differentiation threshold (Figure 16 and 18).

Consistent with these results, depletion of LIF for 24 h caused a metabolic shift from glycolysis to oxidative phosphorylation in E14 Flag-Mock cells but did not cause any significant changes in lactate production rate, ECAR, or OCR levels in E14 Flag-Hk2&Pkm2 cells (Figure 17). E14 Flag-Hk2&Pkm2 cells also experienced a delay in differentiation versus E14 Flag-Mock cells when they were differentiated via EB formation or by RA (Figure 19). Overall, these data suggest that the overexpression of Hk2 and Pkm2 maintains high glycolytic flux during ESC differentiation and delays ESC differentiation.

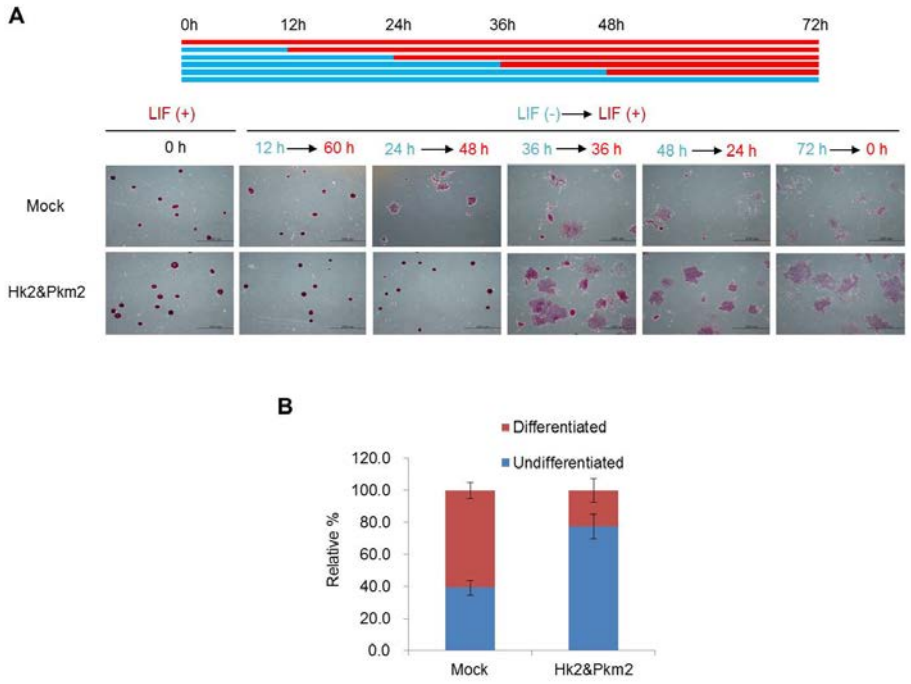

Figure 16. Overexpression of Hk2 and Pkm2 delays ESC differentiation.

(**A**) Overexpression of Hk2 and Pkm2 retards ESC differentiation. E14 cells cultured in serum plus LIF were plated for self-renewal assay. After withdrawal and re-addition of LIF at the indicated time points, the undifferentiated state was assessed by AP staining. (**B**) Increases in Hk2 and Pkm2 levels reduce the ratio of differentiated colony compared with normal cells. The percentage of undifferentiated and differentiated colonies is shown. Values represent mean ± standard deviation (n≥3).

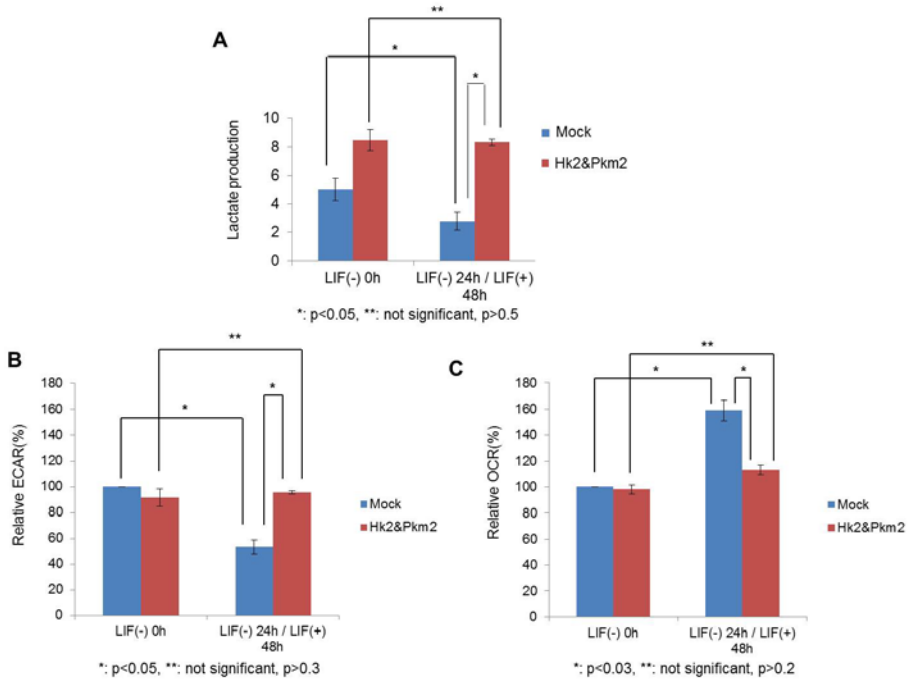

Figure 17. Overexpression of Hk2 and Pkm2 maintains high glycolytic flux under differentiation condition.

(**A**) E14 cells overexpressing Hk2 and Pkm2 retain lactate production, whereas wild-type cells have lower rates. Values represent mean ± standard deviation ($n \geq 3$). (**B and C**) Relative ECAR and OCR rates between normal and Hk2/Pkm2-overexpressing E14 cells. Depletion of LIF for 24 hours did not cause any significant changes in ECAR or OCR level in overexpressing cells. Values represent mean ± standard deviation ($n \geq 3$).

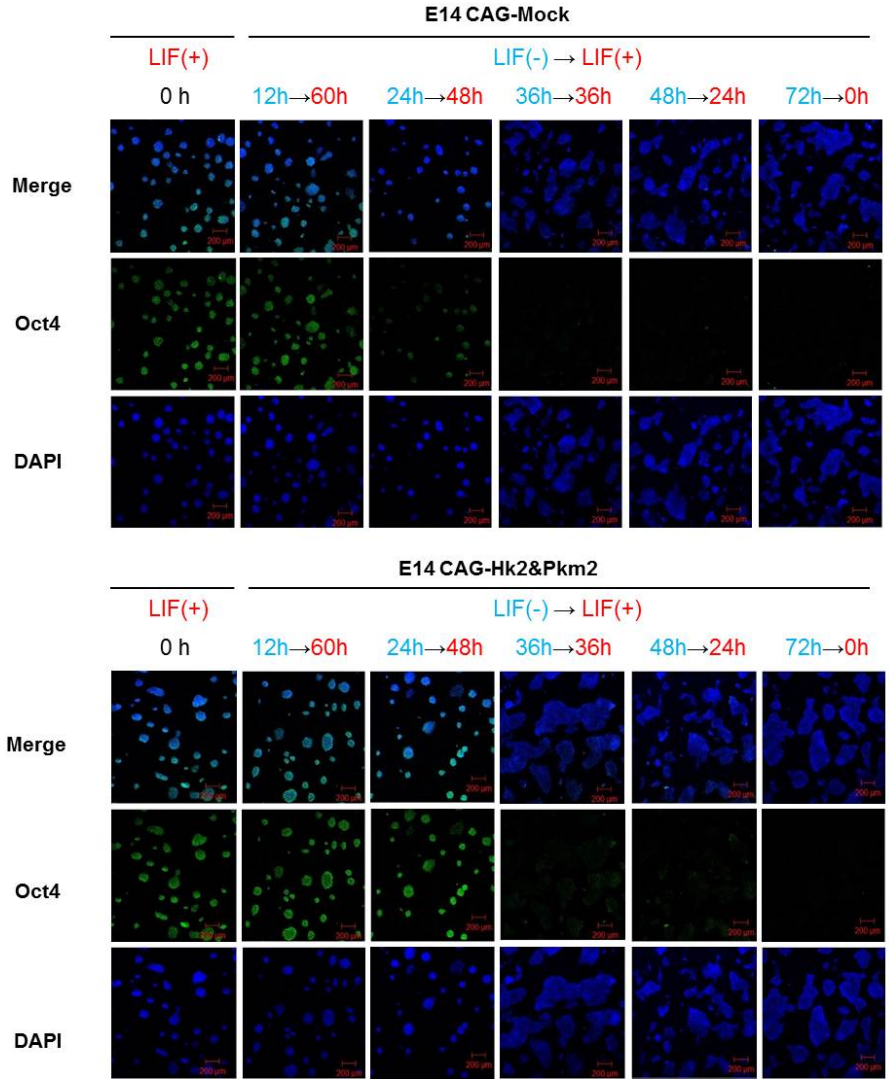
E14 CAG-Mock
LIF(+)
LIF(-) → LIF(+)
0 h
12h→60h
24h→48h
36h→36h
48h→24h
72h→0h
Merge
Oct4
DAPI
E14 CAG-Hk2&Pkm2
LIF(+)
LIF(-) → LIF(+)
0 h
12h→60h
24h→48h
36h→36h
48h→24h
72h→0h
Merge
Oct4
DAPI

Figure 18. E14 ESCs differentiation is delayed upon LIF withdrawal by Hk2 and Pkm2 overexpression.

After withdrawal and re-addition of LIF at the indicated time points, the undifferentiated state was assessed by Oct4-immunostaining. In the 24 hours' time point Oct4 was highly expressed in overexpressing cells rather than control cells.

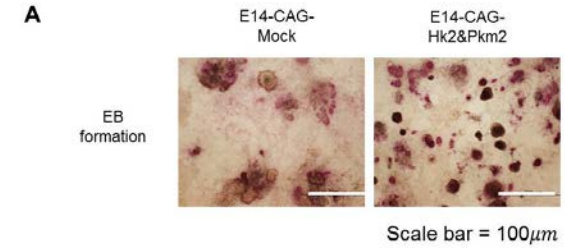
A
E14-CAG-Mock
E14-CAG-Hk2&Pkm2
EB formation
Scale bar = 100μm

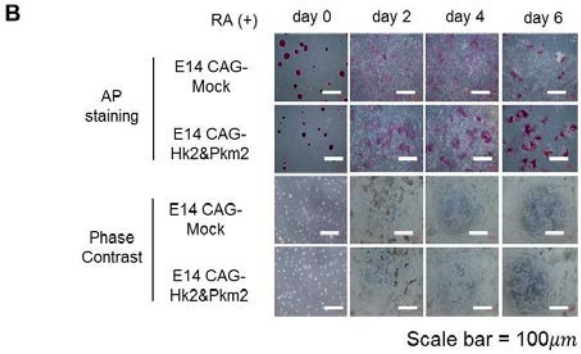
B
RA (+)
day 0
day 2
day 4
day 6
AP staining
E14 CAG-Mock
E14 CAG-Hk2&Pkm2
Phase Contrast
E14 CAG-Mock
E14 CAG-Hk2&Pkm2
Scale bar = 100μm

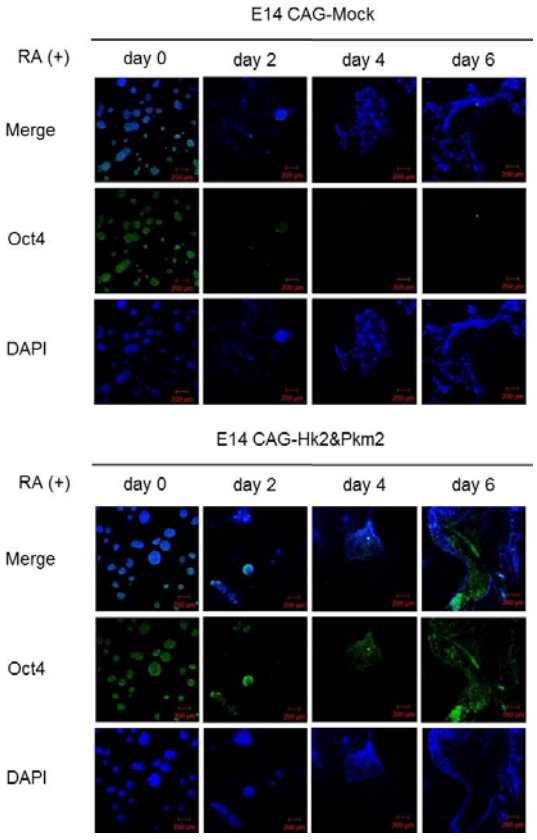
E14 CAG-Mock
RA (+)
day 0
day 2
day 4
day 6
Merge
Oct4
DAPI
E14 CAG-Hk2&Pkm2
RA (+)
day 0
day 2
day 4
day 6
Merge
Oct4
DAPI

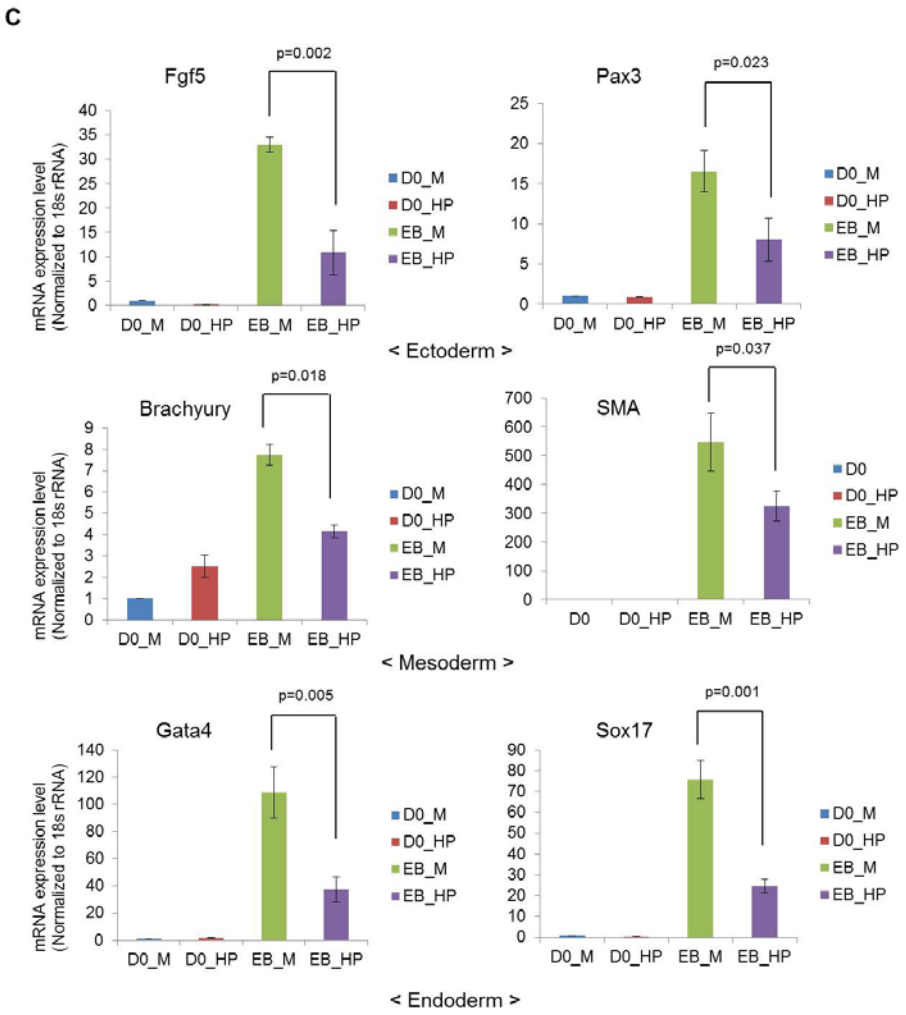
C
Fgf5
p=0.002
mRNA expression level (Normalized to 18s rRNA)
D0_M
D0_HP
EB_M
EB_HP
Pax3
p=0.023
< Ectoderm >
Brachyury
p=0.018
SMA
p=0.037
D0
< Mesoderm >
Gata4
p=0.005
Sox17
p=0.001
< Endoderm >

Figure 19. Overexpression of Hk2 and Pkm2 delays ESCs differentiation via embryoid body (EB) formation or by retinoic acid (RA).

(**A**) For EB formation ESCs dissociated from colonies are transferred into suspension cultures, in which ES cells are allowed to aggregate and form spherical three-dimensional structures EBs. After 8 days, suspension cultured EB was reattached on gelatin-coated culture plates, and keep them in attached about 2 weeks for further differentiation and then stained with AP. (**B**) For RA mediated differentiations, ESCs were cultured on gelatin-coated plates in serum-containing ESC medium without LIF. After 2 days, the medium was replaced with serum-free neural differentiation medium, composed of serum-free N2B27 medium that was supplemented with RA (10nM), and cultured for 6 additional days. After addition of RA at the indicated time points, the undifferentiated state was assessed by AP staining and Oct4-immunostaining. (**C**) Representative 3 germ layer marker genes were analyzed by real-time qPCR. Relative mRNA expression levels are expressed as mean $\pm$ standard deviation ($n \geq 3$).

4. Sustaining high glycolysis levels enables some population of ESCs to retain self-renewal and differentiation potential in the absence of LIF

On withdrawal of LIF, ESCs generally lost pluripotency within several days, showing flattened morphology, and were not positive for AP or Oct4. Eventually, they lost their potential for self-renewal and could not be maintained for long periods. However, certain populations of E14 Flag-Hk2&Pkm2 cells maintained an undifferentiated ESC-like morphology and were positive for AP staining and Oct4 by immunostaining, even ~2 weeks after LIF withdrawal (Figure 21A). These cells were dissimilar to undifferentiated ESCs, because they expressed Oct4 but little or no Sox2 and Nanog (Figure 20). These results showed that sustaining high glycolysis by overexpression of both Hk2 and Pkm2 hampers full differentiation of ESCs in the absence of LIF for a long time.

However, they retained their capacity for self-renewal (or immortality), such that E14 Flag-Hk2&Pkm2 cells could be maintained for several months in the absence of LIF (Figure 21 B-D). E14 Flag-Hk2&Pkm2 cells that have been LIF-deprived for the long term were positive for AP, and approximately 80% of cells were positive for SSEA1 by flow cytometry (Figure 21 B-D). Long-term LIF deprivation of E14 Flag-Hk2&Pkm2 cells allowed them to retain some differentiation potential, forming teratomas that comprised ectoderm, mesoderm, and endoderm cells when they were transplanted to SCID mice (Figure 21E). These results show that sustaining high glycolysis levels by overexpression of Hk2 and Pkm2 enables ESCs to retain self-

renewal mechanisms and some differentiation potential in the absence of LIF.

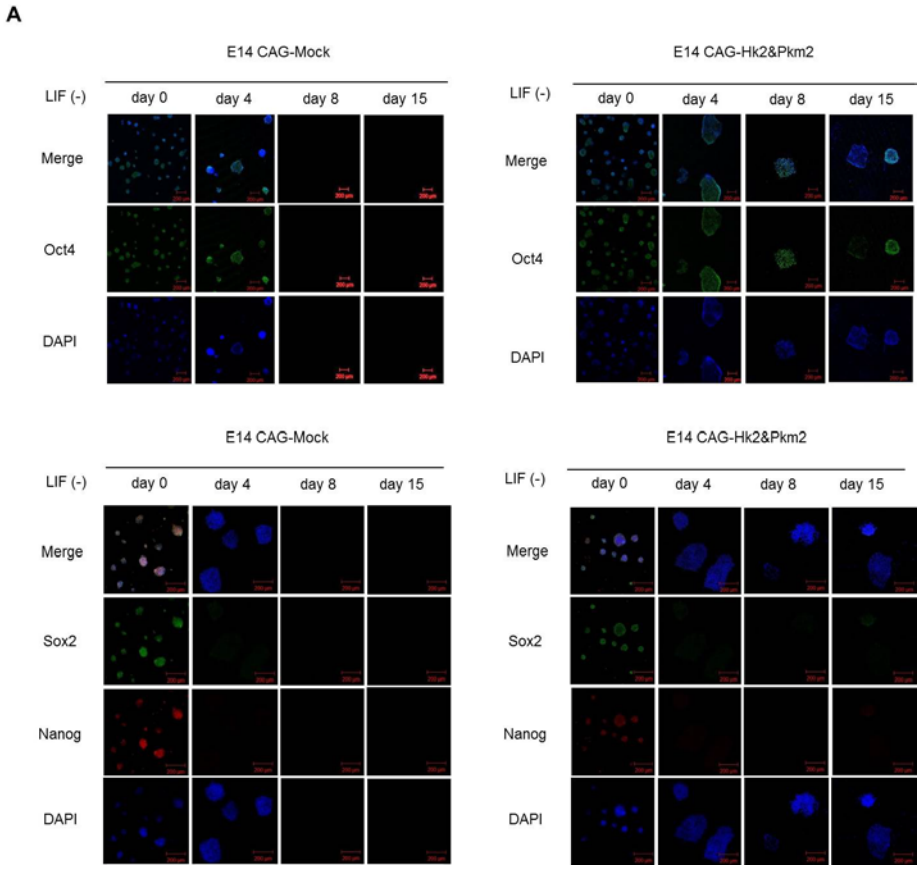

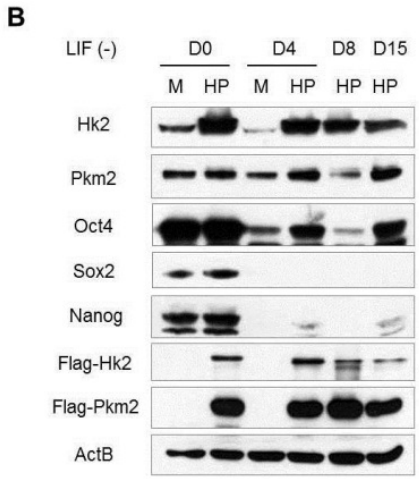

M: E14 CAG-Mock
HP: E14 CAG-Hk2&Pkm2

Figure 20. E14 Flag-Hk2&Pkm2 cells maintain Oct4 expression in the absence of LIF.

E14 Flag-Hk2&Pkm2 cells were maintained in the absence of LIF. The changes in protein levels of Oct4, Sox2, and Nanog during LIF withdrawal were determined by (**A**) immunostaining and confocal microscopy or (**B**) by Western blot. E14 Flag-Hk2&Pkm2 cells were different to general undifferentiated stem cells, because they expressed Oct4 but little or no Sox2 and Nanog.

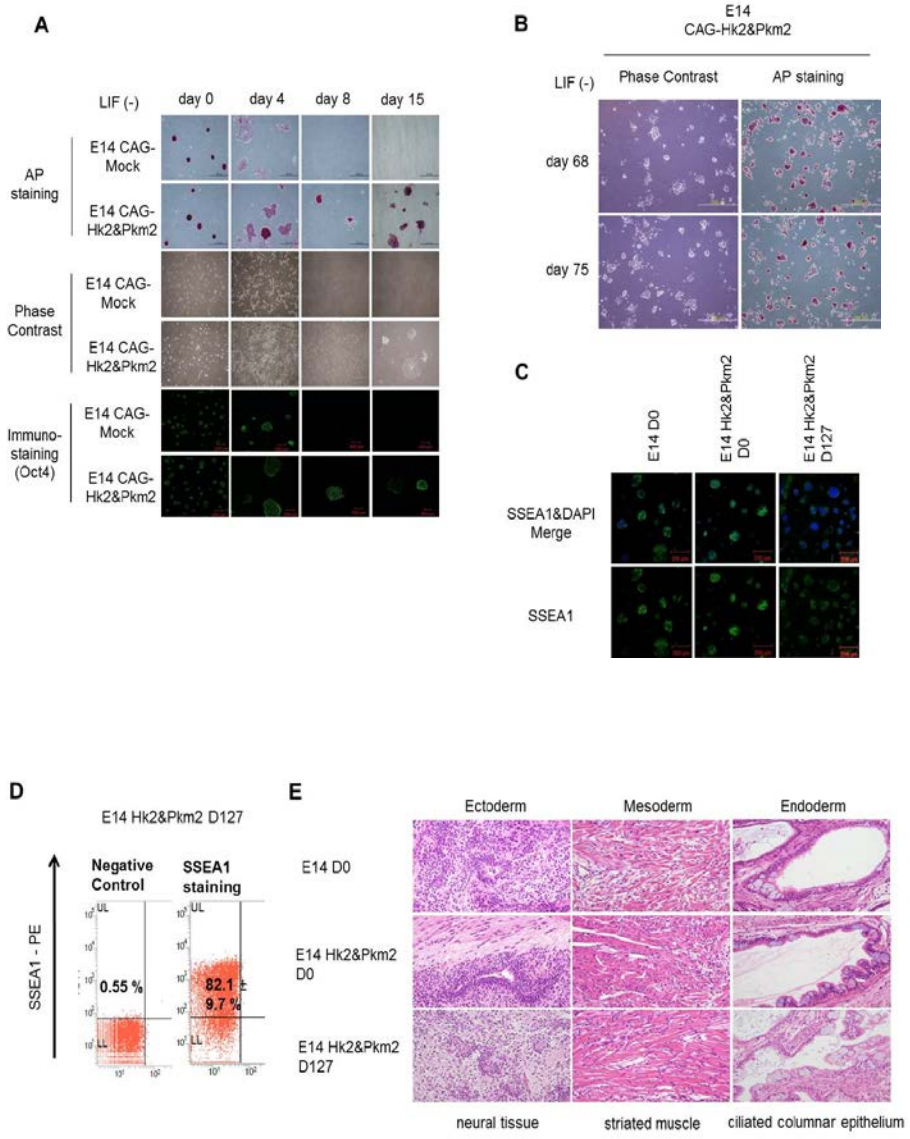
A
LIF (-)
day 0
day 4
day 8
day 15
AP staining
E14 CAG-Mock
E14 CAG-Hk2&Pkm2
Phase Contrast
E14 CAG-Mock
E14 CAG-Hk2&Pkm2
Immuno-staining (Oct4)
E14 CAG-Mock
E14 CAG-Hk2&Pkm2
B
E14
CAG-Hk2&Pkm2
LIF (-)
Phase Contrast
AP staining
day 68
day 75
C
E14 D0
E14 Hk2&Pkm2 D0
E14 Hk2&Pkm2 D127
SSEA1&DAPI Merge
SSEA1
D
E14 Hk2&Pkm2 D127
Negative Control
SSEA1 staining
SSEA1 - PE
UL
LL
0.55 %
82.1 ± 9.7 %
E
Ectoderm
Mesoderm
Endoderm
E14 D0
E14 Hk2&Pkm2 D0
E14 Hk2&Pkm2 D127
neural tissue
striated muscle
ciliated columnar epithelium

Figure 21. Sustaining high glycolysis levels enables some population of ESCs to retain self-renewal and differentiation potential in the absence of LIF.

(**A**) Continuous culture of Hk2- and Pkm2-overexpressing E14 ESCs in the absence of LIF; the cells were maintained and cultured for up to 15 days. The undifferentiated state was assessed by AP staining. (**B and C**) Hk2- and Pkm2-overexpressing E14 cells can be maintained for more than 2 months in the absence of LIF. (**D**) FACS sorting analysis showed that more than 80 % of E14 Hk2&Pkm2 cells were positive to SSEA1 (stem cell surface marker). (**E**) SCID mice were transplanted with E14 D0, E14 Hk2&Pkm2 D0, and E14 Hk2&Pkm2 D40 cells. After 6–8 weeks, the subcutaneous teratomas were dissected and stained with hematoxylin and eosin.

5. Molecular signature of an ESC derivative sustaining high glycolysis levels in the absence of LIF

Because long-term LIF-deprived E14 Flag-Hk2&Pkm2 cells had a normal karyotype (Figure 22A) and retained the capacity for self-renewal and some differentiation potential (Figure 21), we examined whether these cells were similar to other pluripotent stem cells, such as epiblast stem cells (EpiSCs), Epiblast-like cells (EpiLCs), and early primitive ectoderm-like (EPL) cells (57-59). We used Dnmt3b and Wnt3 as markers for EpiSCs and EpiLCs and Rex1 as an EPL cell marker. Long-term LIF-deprived E14 Flag-Hk2&Pkm2 cells expressed all markers at distinct levels, suggesting they were not identical to any of these pluripotent stem cells (Figure 22B).

To characterize long-term LIF-deprived E14 Flag-Hk2&Pkm2 cells, we sequenced RNA from cells that were grown for 40 days in the absence of LIF (E14 Hk2&Pkm2 D40). As a control, we used the RNA sequencing data of E14 cells in the presence of LIF (E14 D0) and in the absence of LIF for 7 days (E14 D7) and E14 Flag-Hk2&Pkm2 cells that were maintained with LIF (E14 Flag-Hk2&Pkm2 D0). In this comparison of whole-gene expression profiles, E14 Flag-Hk2&Pkm2 D0 cells were nearly identical to E14 D0 cells and E14 Flag-Hk2&Pkm2 D40 cells closely resembled E14 D0 cells (Figure 22C and 22D). Although the levels of certain pluripotency-related genes were similar between E14 Flag-Hk2&Pkm2 D40 and E14 D0 cells, differences remained, especially in the levels of Sox2 and Nanog (Figure 22D).

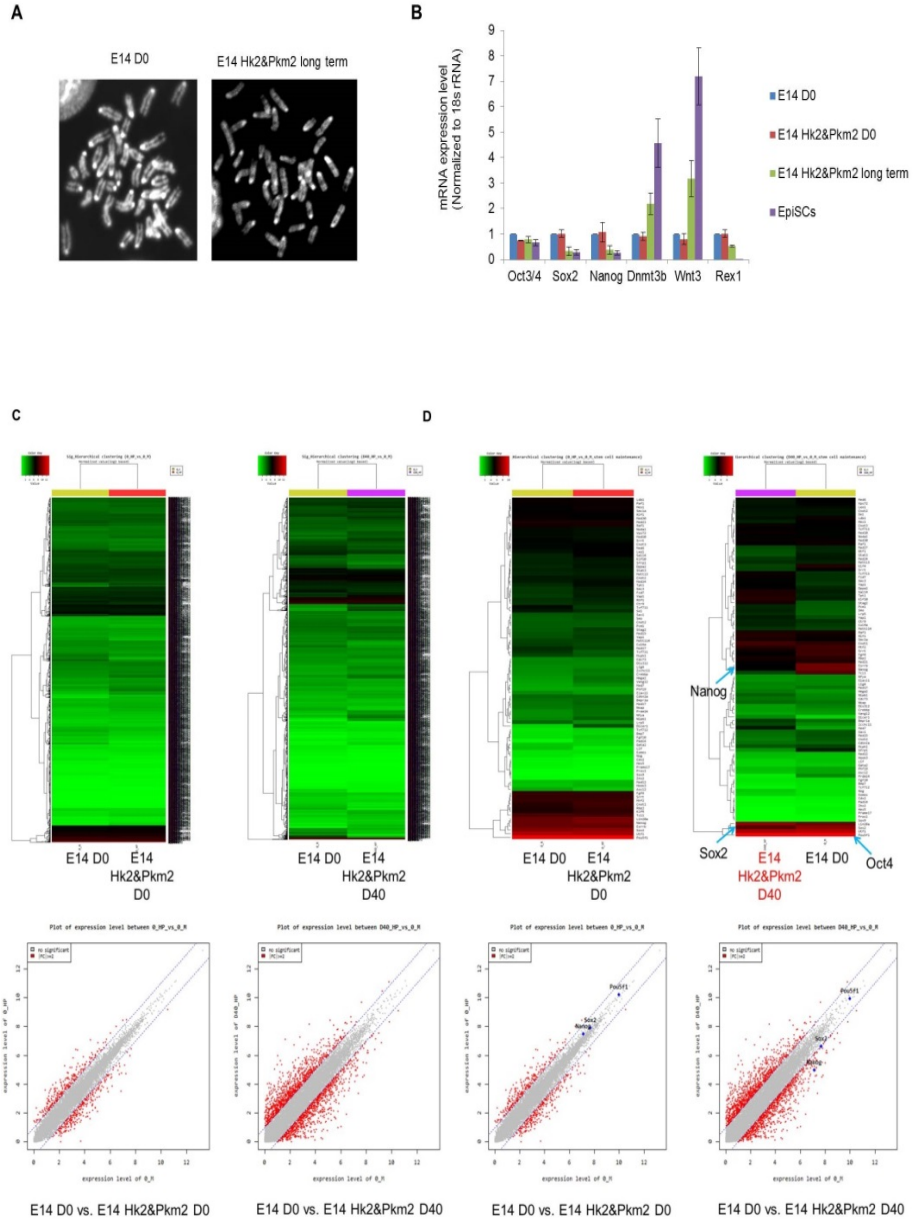
A
E14 D0
E14 Hk2&Pkm2 long term
B
mRNA expression level
(Normalized to 18s rRNA)
E14 D0
E14 Hk2&Pkm2 D0
E14 Hk2&Pkm2 long term
EpiSCs
Oct3/4
Sox2
Nanog
Dnmt3b
Wnt3
Rex1
C
D
E14 D0
E14 Hk2&Pkm2 D0
E14 Hk2&Pkm2 D40
Nanog
Sox2
Oct4
E14 Hk2&Pkm2 D40
E14 D0 vs. E14 Hk2&Pkm2 D0
E14 D0 vs. E14 Hk2&Pkm2 D40
E14 D0 vs. E14 Hk2&Pkm2 D0
E14 D0 vs. E14 Hk2&Pkm2 D40

Figure 22. Molecular signature of long-term LIF deprived E14 Flag-Hk2&Pkm2 cells

(**A**) Karyotype of E14 Mock and long-term LIF deprived E14 Flag-Hk2&Pkm2 cells. (**B**) The marker genes expression levels in E14 Flag-Hk2&Pkm2 cells for various pluripotent states (EpiSCs, EpiLCs, and EPL cell) were determined by RT-PCR and real-time qPCR. Dnmt3b and Wnt3 were used as markers for EpiSCs and EpiLCs and Rex1 as an EPL cell marker. (**C**) Whole gene expression analysis between E14 D0 and E14 Hk2&Pkm2 D40 cells. (**D**) Pluripotency related gene expression analysis between E14 D0 and E14 Hk2&Pkm2 D40 cells. The levels of certain pluripotency-related genes were similar between E14 Flag-Hk2&Pkm2 D40 and E14 D0 cells. However, differences remained, especially in the levels of Sox2 and Nanog.

In the comparison of RNA-seq data of the 3 conditions, certain gene sets were downregulated during ESC differentiation, some subsets of which were reactivated in E14 Hk2&Pkm2 D40 cells. Similarly, several gene sets were upregulated during ESC differentiation, certain subsets of which were re-repressed in E14 Hk2&Pkm2 D40 cells (Figure 23A). We grouped genes that were up- and downregulated during ESC differentiation and reactivated and re-repressed in E14 Hk2&Pkm2 D40 cells (Figure 23B).

Many genes that were related to differentiation, senescence, and apoptosis underwent upregulation during differentiation and re-repression in Hk2- and Pkm2- overexpressing cells, whereas those that were downregulated during differentiation and reactivated were involved in proliferation and the cell cycle (Figure 23 and 24). These results suggest that sustaining high glycolysis levels by overexpression of Hk2 and Pkm2 impedes differentiation, senescence, and apoptosis; thus, ESCs retain the capacity for self-renewal and some differentiation potential in the absence of LIF.

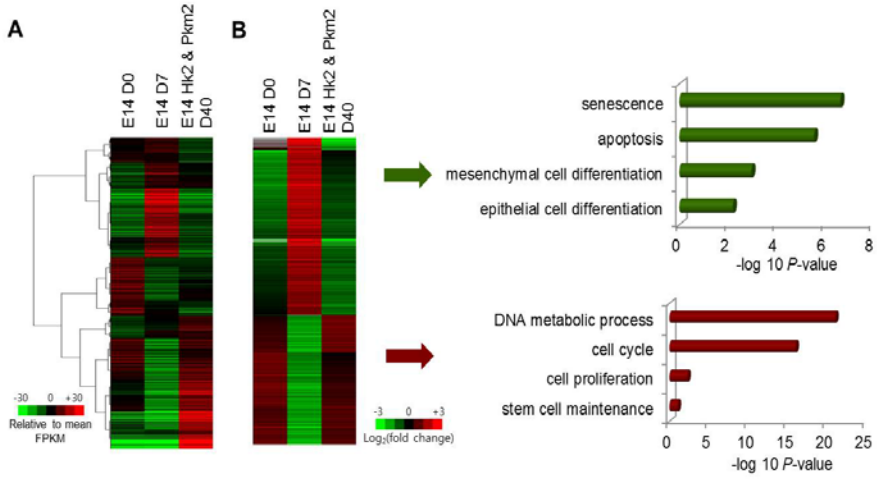
A
E14 D0
E14 D7
E14 Hk2 & Pkm2 D40
-30 0 +30
Relative to mean FPKM
B
E14 D0
E14 D7
E14 Hk2 & Pkm2 D40
-3 0 +3
Log2(fold change)
senescence
apoptosis
mesenchymal cell differentiation
epithelial cell differentiation
0 2 4 6 8
-log 10 P-value
DNA metabolic process
cell cycle
cell proliferation
stem cell maintenance
0 5 10 15 20 25
-log 10 P-value

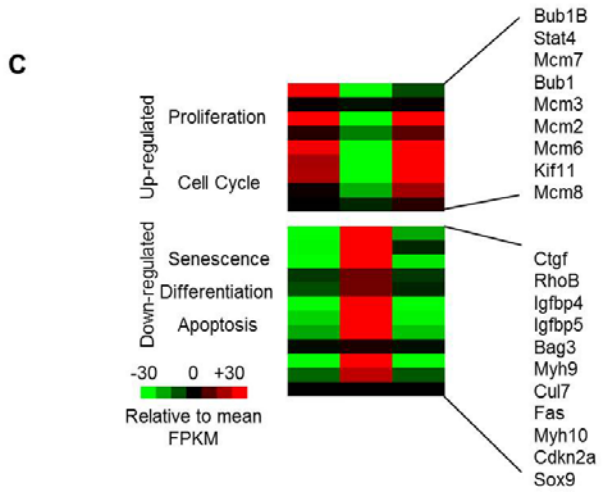
C
Up-regulated
Proliferation
Cell Cycle
Down-regulated
Senescence
Differentiation
Apoptosis
-30 0 +30
Relative to mean FPKM
Bub1B
Stat4
Mcm7
Bub1
Mcm3
Mcm2
Mcm6
Kif11
Mcm8
Ctgf
RhoB
Igfbp4
Igfbp5
Bag3
Myh9
Cul7
Fas
Myh10
Cdkn2a
Sox9

Figure 23. Molecular signature of an ESC derivative sustaining high glycolysis in the absence of LIF.

(**A**) Hierarchical clustering images of genes altered in E14 cells in the presence of LIF (E14 D0) and in the absence of LIF for 7 days (E14 D7) and in Hk2- and Pkm2-overexpressing cells grown for 40 days in the absence of LIF (E14 Hk2 & Pkm2 D40). (**B**) Some functional categories of genes were significantly enriched in response to Hk2 and Pkm2 overexpression. Analyses were performed with significantly up- or downregulated genes by Hk2 and Pkm2, respectively, using DAVID. (**C**) Representative up- and downregulated genes in E14 Hk2 and Pkm2 D40 cells compared with E14 D7 cells, related to proliferation, cell cycle, senescence, and apoptosis.

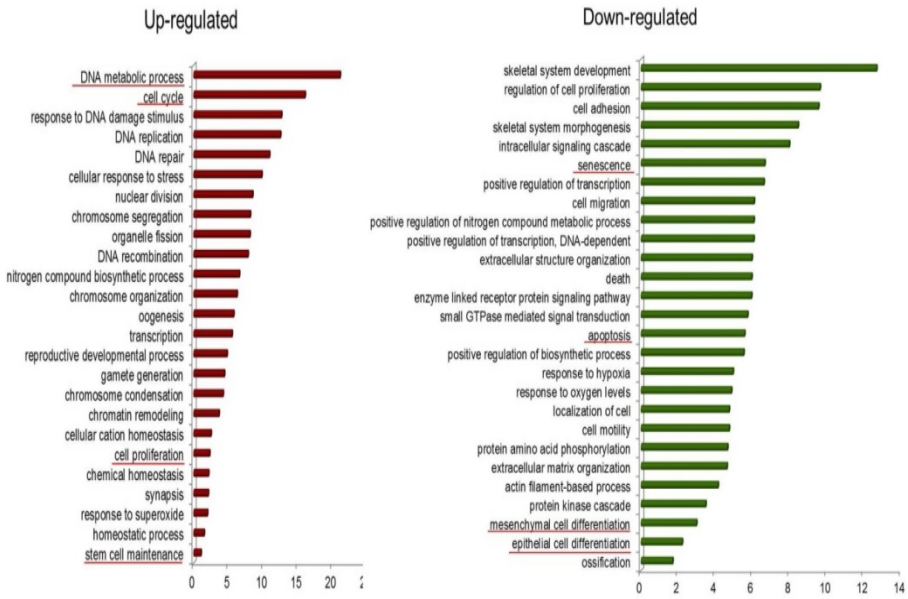

Figure 24. Gene ontology analysis of the genes in Hk2 and Pkm2 overexpressed cell.

Gene ontology analysis of the genes that was up-regulated or down-regulated in Hk2 and Pkm2 overexpressed cell. In Hk2 and Pkm2 overexpressed cells that were maintained without LIF, the genes related to cell cycle and proliferations were up-regulated while senescence, differentiation, and apoptosis related genes were down-regulated.

Overall, our results demonstrate that Oct4 directly regulates Hk2 and Pkm2 to maintain high glycolytic flux in ESCs. During normal ESC differentiation, glycolytic flux is downregulated. Glycolytic flux affects stemness—the continuation of high glycolysis levels during ESC differentiation prevents ESCs from differentiating completely. The resulting cells escaped from senescence and apoptosis, allowing them to retain self-renewal potential or immortality (Figure 25).

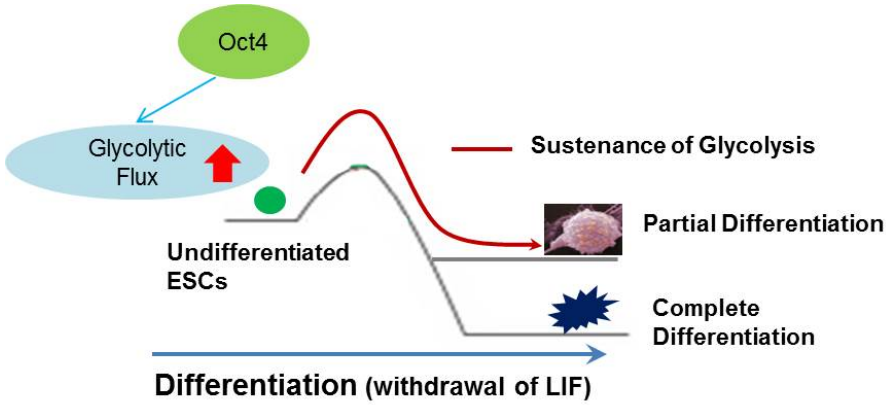

Figure 25. A summary model.

Oct4 directly regulates Hk2 and Pkm2 to maintain high glycolytic flux in ESCs. Sustaining high glycolysis during ESC differentiation retards ESCs, preventing them from undergoing complete differentiation. The resulting cells escape from senescence and apoptosis and might retain pluripotency.

4. DISCUSSION

One outstanding issue in stem cell biology is whether stemness factors drive specific cellular functions, such as metabolism, in a specific manner to maintain stemness (5). In this study, we demonstrated that Oct4 directly regulates the key glycolytic enzymes Hk2 and Pkm2. Based on our ChIP-seq and conventional ChIP-real time qPCR results, Oct4 binds to the Hk2 and Pkm2 genes (Figure 6 and 12A). By reporter gene assay, Oct4 regulated the promoter activity of Hk2 and Pkm2 (Figure 12B and 12C). Consequently, Oct4 governed the expression of Hk2 and Pkm2 mRNA in 3 systems (Figure 8 and 9), and Hk2 and Pkm2 mRNA levels reflected their protein levels (Figure 10).

Although we did not completely examine the contribution of other pluripotency factors to the regulation of ESC metabolism, it is likely that Sox2 and Nanog also participate in regulating glycolysis. The ChIP-seq results clearly showed that OSN occupied the Hk2 and Pkm2 genes (Figure 11A)—OSN usually functions together in the active promoters in ESCs (60). Thus, our study suggests that core pluripotency factors regulate the transcriptional network of pluripotency and ESC metabolism.

Recently, many studies have proposed the metabolic regulation of stemness (3, 18, 36, 37, 39). Although it is clear that high glycolysis levels are important for pluripotency, their impact on stemness remains unknown. In this report, we artificially sustained high glycolysis during ESC differentiation by overexpressing Hk2 and Pkm2, enabling certain ESC populations to maintain the capacity for self-renewal and some differentiation potential in the absence of LIF (Figure 13, 14, and 21).

Consistent with findings that the senescence-related mitochondrial/oxidative stress pathway is activated during PSC differentiation (33), our RNA-seq results showed that various genes in apoptosis and senescence were upregulated on withdrawal of LIF in ESCs (Figure 23). Overexpression of Hk2 and Pkm2 downregulated apoptosis- and senescence-related genes and upregulated genes that are involved in cell proliferation and the cell cycle (Figure 23), maintaining self-renewal potential in the absence of LIF.

Moreover, Hk2- and Pkm2-overexpressing cells retained some pluripotency-related genes, such as Oct4, in the absence of LIF, allowing them to maintain some differentiation potential (Figure 20 and 21). Our study suggests that the upregulation of glycolytic flux drives some ESC cells to maintain self-renewal and the potential for differentiation; consistent with this model, previous overexpression of phosphoglycerate mutase increases glycolytic flux and enables mouse fibroblasts to escape from replicative senescence(61) and early induction of HIF-1 alpha targets increased glycolytic flux and enhanced reprogramming of dermal fibroblasts to iPSCs (47).

Our experimental results showed that E14 Flag-Hk2& Pkm2 cells maintained considerable level of Oct4, self-renewal potential and retained pluripotency in the absence of LIF (Figure 21). Previous reports suggested some molecular link between Hk2, Pkm2 and Oct4. Hk2 has been identified as a protein binds to Oct4 in wild type linker domain dependent manner which that is crucial in reprogramming (62). Pkm2 has been reported to interact with

Oct4 POU DNA binding domain via its C-terminal region and enhances Oct4-mediated transcription (63). Because overexpression of single Hk2 or Pkm2 did not enhanced glycolytic flux and did not allow ESCs to be maintained in the long absence of LIF (data not shown), cooperation between Hk2, Pkm2 and high glycolytic flux may be critical in this mechanism.

The E14 Hk2&Pkm2 cells that were cultured without LIF were apparently not normal undifferentiated ESCs, although they were positive for alkaline phosphatase and SSEA1 (Figure 21A-21C). They expressed Sox2 and Nanog at a similar level to EpiSCs. Moreover, Dnmt3b, Wnt3, and Rex1 levels of E14 Hk2&Pkm2 cells were intermediate state between ESCs and EpiSCs (Figure 22B). Therefore, it is possible to suggest that long-term LIF-deprived E14 Flag-Hk2&Pkm2 cells exist in an intermediate state between ESCs and EpiSCs. In addition, E14 Hk2&Pkm2 cells could be maintained LIF independently for several months and could form teratomas, comprising the 3 germ layers, which resembled some characteristics of cancer stem cells.

The glucose and lactate levels in cancer cells rise in a well-oxygenated environment through a process, known as the Warburg effect. Hk2 and Pkm2 mediate tumorigenesis per the Warburg effect (64, 65). In the Warburg effect, cancer cells are thought to shunt glycolytic intermediates into amino acid, lipid and nucleotide synthesis for cell proliferation (30). Similarly, mouse ESCs show increased activity of the PPP, demonstrating that anabolic glycolysis is a common feature of metabolism in both ESCs and cancer cells

(5). Such increased aerobic glycolysis has been observed in a variety of cancer types. Although whether this metabolic switch in cancer cells is a causal event in cancer development or merely a downstream biochemical symptom of cancer remains a matter of debate, accumulating evidences seem to suggest that aerobic glycolysis is closely associated with tumorigenesis and plays important roles in maintaining the malignant behaviors of the cancer cells and promoting metastasis (66). High levels of glycolysis seem to confer survival advantage to malignant cells in hypoxic or acidosis microenvironments during cancer development. This unique metabolic profile of cancer cells provides a biochemical basis for developing new chemotherapeutic strategies targeting the glycolysis pathway in cancer cells (67).

The high glycolytic activity in cancer tissues requires upregulation of the key glycolytic enzymes, including Hk2 and Pkm2. Knockdown of PKM2 in a panel of cancer cell lines reduced glucose uptake, increased oxygen consumption, and decreased lactate production; these changes were reversed when PKM2 was reintroduced, but not on PKM1 re-introduction (68). Furthermore, re-expression of PKM2 promoted cell proliferation and xenograft tumor formation, unlike cells in which PKM1 was re-expressed (65). Hk2 is highly expressed in lung and breast cancers, and Pkm2 is highly expressed in colon, breast, lung, and cervical cancers, all of which have poor prognosis (68-70). This highlights the need for further study on the significance of Hk2 and Pkm2 in ESCs and cancer cells. Due to the frequent

up-regulation of Hk2 and Pkm2 in cancer cells and their important role in the glycolytic pathway, these enzymes seem to be attractive targets for the development of anticancer drugs.

5. REFERENCES

1. Ng HH, Surani MA. The transcriptional and signalling networks of pluripotency. Nature cell biology. 2011;13(5):490-6.

2. Hanna JH, Saha K, Jaenisch R. Pluripotency and cellular reprogramming: facts, hypotheses, unresolved issues. Cell. 2010;143(4):508-25.

3. Folmes CD, Dzeja PP, Nelson TJ, Terzic A. Metabolic plasticity in stem cell homeostasis and differentiation. Cell stem cell. 2012;11(5):596-606.

4. Zhang J, Nuebel E, Daley GQ, Koehler CM, Teitell MA. Metabolic regulation in pluripotent stem cells during reprogramming and self-renewal. Cell stem cell. 2012;11(5):589-95.

5. Shyh-Chang N, Daley GQ, Cantley LC. Stem cell metabolism in tissue development and aging. Development. 2013;140(12):2535-47.

6. Metallo CM, Vander Heiden MG. Metabolism strikes back: metabolic flux regulates cell signaling. Genes & development. 2010;24(24):2717-22.

7. Lu C, Thompson CB. Metabolic regulation of epigenetics. Cell metabolism. 2012;16(1):9-17.

8. Barbehenn EK, Wales RG, Lowry OH. Measurement of metabolites in single preimplantation embryos; a new means to study metabolic control in early embryos. Journal of embryology and experimental morphology. 1978;43:29-46.

9. Quinn P, Wales RG. Adenosine triphosphate content of preimplantation mouse embryos. Journal of reproduction and fertility. 1971;25(1):133-5.

10. Johnson MT, Mahmood S, Patel MS. Intermediary metabolism and energetics during murine early embryogenesis. The journal of biological chemistry. 2003;278(34):31457-60.

11. Graves CN, Biggers JD. Carbon dioxide fixation by mouse embryos prior to implantation. Science. 1970;167(3924):1506-8.

12. Leese HJ, Barton AM. Pyruvate and glucose uptake by mouse ova and preimplantation embryos. Journal of reproduction and fertility. 1984;72(1):9-13.

13. Zhang J, Khvorostov I, Hong JS, Oktay Y, Vergnes L, Nuebel E, et al. UCP2 regulates energy metabolism and differentiation potential of human pluripotent stem cells. The EMBO journal. 2011;30(24):4860-73.

14. Wang J, Alexander P, Wu L, Hammer R, Cleaver O, McKnight SL. Dependence of mouse embryonic stem cells on threonine catabolism. Science. 2009;325(5939):435-9.

15. Cho YM, Kwon S, Pak YK, Seol HW, Choi YM, Park do J, et al. Dynamic changes in mitochondrial biogenesis and antioxidant enzymes during the spontaneous differentiation of human embryonic stem cells. Biochemical and biophysical research communications. 2006;348(4):1472-8.

16. Chung S, Dzeja PP, Faustino RS, Perez-Terzic C, Behfar A, Terzic A. Mitochondrial oxidative metabolism is required for the cardiac differentiation of stem cells. Nature clinical practice cardiovascular medicine. 2007;4 Suppl 1:S60-7.

17. Facucho-Oliveira JM, Alderson J, Spikings EC, Egginton S, St John JC. Mitochondrial DNA replication during differentiation of murine embryonic stem cells. Journal of cell science. 2007;120(Pt 22):4025-34.

18. Yanes O, Clark J, Wong DM, Patti GJ, Sanchez-Ruiz A, Benton HP, et al. Metabolic oxidation regulates embryonic stem cell differentiation. Nature chemical biology. 2010;6(6):411-7.

19. Leese HJ. Metabolism of the preimplantation embryo: 40 years on. Reproduction. 2012;143(4):417-27.

20. Brinster RL, Troike DE. Requirements for blastocyst development in vitro. Journal of animal science. 1979;49 Suppl 2:26-34.

21. Jansen S, Pantaleon M, Kaye PL. Characterization and regulation of monocarboxylate cotransporters Slc16a7 and Slc16a3 in preimplantation mouse embryos. Biology of reproduction. 2008;79(1):84-92.

22. Martin KL, Leese HJ. Role of glucose in mouse preimplantation embryo development. Molecular reproduction and development. 1995;40(4):436-43.

23. Carey BW, Finley LW, Cross JR, Allis CD, Thompson CB. Intracellular alpha-ketoglutarate maintains the pluripotency of embryonic stem cells. Nature. 2015;518(7539):413-6.

24. Moussaieff A, Kogan NM, Aberdam D. Concise Review: Energy Metabolites: Key Mediators of the Epigenetic State of Pluripotency. Stem cells. 2015;33(8):2374-80.

25. Ryall JG, Dell'Orso S, Derfoul A, Juan A, Zare H, Feng X, et al. The NAD(+)-dependent SIRT1 deacetylase translates a metabolic switch into regulatory epigenetics in skeletal muscle stem cells. Cell stem cell. 2015;16(2):171-83.

26. Shiraki N, Shiraki Y, Tsuyama T, Obata F, Miura M, Nagae G, et al. Methionine metabolism regulates maintenance and differentiation of human pluripotent stem cells. Cell metabolism. 2014;19(5):780-94.

27. Wellen KE, Hatzivassiliou G, Sachdeva UM, Bui TV, Cross JR, Thompson CB. ATP-citrate lyase links cellular metabolism to histone acetylation. Science. 2009;324(5930):1076-80.

28. Ryall JG, Cliff T, Dalton S, Sartorelli V. Metabolic Reprogramming of Stem Cell Epigenetics. Cell stem cell. 2015;17(6):651-62.

29. Jang H, Yang J, Lee E, Cheong JH. Metabolism in embryonic and cancer stemness. Archives of pharmacal research. 2015;38(3):381-8.

30. Vander Heiden MG, Cantley LC, Thompson CB. Understanding the Warburg effect: the metabolic requirements of cell proliferation. Science. 2009;324(5930):1029-33.

31. Ito K, Suda T. Metabolic requirements for the maintenance of self-renewing stem cells. Nature reviews molecular cell biology. 2014;15(4):243-56.

32. Varum S, Rodrigues AS, Moura MB, Momcilovic O, Easley CAt, Ramalho-Santos J, et al. Energy metabolism in human pluripotent stem cells and their differentiated counterparts. Plos one. 2011;6(6):e20914.

33. Prigione A, Fauler B, Lurz R, Lehrach H, Adjaye J. The senescence-related mitochondrial/oxidative stress pathway is repressed in human induced pluripotent stem cells. Stem cells. 2010;28(4):721-33.

34. Armstrong L, Tilgner K, Saretzki G, Atkinson SP, Stojkovic M, Moreno R, et al. Human induced pluripotent stem cell lines show stress defense mechanisms and mitochondrial regulation similar to those of human embryonic stem cells. Stem cells. 2010;28(4):661-73.

35. Folmes CD, Nelson TJ, Martinez-Fernandez A, Arrell DK, Lindor JZ, Dzeja PP, et al. Somatic oxidative bioenergetics transitions into pluripotency-dependent glycolysis to facilitate nuclear reprogramming. Cell metabolism. 2011;14(2):264-71.

36. Mathieu J, Zhou W, Xing Y, Sperber H, Ferreccio A, Agoston Z, et al. Hypoxia-inducible factors have distinct and stage-specific roles

during reprogramming of human cells to pluripotency. Cell stem cell. 2014;14(5):592-605.

37. Jang H, Kim Tae W, Yoon S, Choi S-Y, Kang T-W, Kim S-Y, et al. O-GlcNAc Regulates Pluripotency and Reprogramming by Directly Acting on Core Components of the Pluripotency Network. Cell stem cell. 2012;11(1):62-74.

38. Zhu S, Li W, Zhou H, Wei W, Ambasudhan R, Lin T, et al. Reprogramming of human primary somatic cells by OCT4 and chemical compounds. Cell stem cell. 2010;7(6):651-5.

39. Panopoulos AD, Yanes O, Ruiz S, Kida YS, Diep D, Tautenhahn R, et al. The metabolome of induced pluripotent stem cells reveals metabolic changes occurring in somatic cell reprogramming. Cell research. 2012;22(1):168-77.

40. Ang YS, Tsai SY, Lee DF, Monk J, Su J, Ratnakumar K, et al. Wdr5 mediates self-renewal and reprogramming via the embryonic stem cell core transcriptional network. Cell. 2011;145(2):183-97.

41. Marson A, Levine SS, Cole MF, Frampton GM, Brambrink T, Johnstone S, et al. Connecting microRNA genes to the core

transcriptional regulatory circuitry of embryonic stem cells. Cell. 2008;134(3):521-33.

42. Whyte WA, Orlando DA, Hnisz D, Abraham BJ, Lin CY, Kagey MH, et al. Master transcription factors and mediator establish super-enhancers at key cell identity genes. Cell. 2013;153(2):307-19.

43. Thomson M, Liu SJ, Zou LN, Smith Z, Meissner A, Ramanathan S. Pluripotency factors in embryonic stem cells regulate differentiation into germ layers. Cell. 2011;145(6):875-89.

44. Han DW, Greber B, Wu G, Tapia N, Arauzo-Bravo MJ, Ko K, et al. Direct reprogramming of fibroblasts into epiblast stem cells. Nature cell biology. 2011;13(1):66-71.

45. Niwa H, Masui S, Chambers I, Smith AG, Miyazaki J. Phenotypic complementation establishes requirements for specific POU domain and generic transactivation function of Oct-3/4 in embryonic stem cells. Molecular and cellular biology. 2002;22(5):1526-36.

46. Niwa H, Miyazaki J, Smith AG. Quantitative expression of Oct-3/4 defines differentiation, dedifferentiation or self-renewal of ES cells. Nature genetics. 2000;24(4):372-6.

47. Prigione A, Rohwer N, Hoffmann S, Mlody B, Drews K, Bukowiecki R, et al. HIF1alpha modulates cell fate reprogramming through early glycolytic shift and upregulation of PDK1-3 and PKM2. Stem cells. 2014;32(2):364-76.

48. Kim JH, Shim J, Ji MJ, Jung Y, Bong SM, Jang YJ, et al. The condensin component NCAPG2 regulates microtubule-kinetochore attachment through recruitment of Polo-like kinase 1 to kinetochores. Nature communications. 2014;5:4588.

49. Trapnell C, Pachter L, Salzberg SL. TopHat: discovering splice junctions with RNA-Seq. Bioinformatics. 2009;25(9):1105-11.

50. Roberts A, Trapnell C, Donaghey J, Rinn JL, Pachter L. Improving RNA-Seq expression estimates by correcting for fragment bias. Genome biology. 2011;12(3):R22.

51. Anders S, Huber W. Differential expression analysis for sequence count data. Genome biology. 2010;11(10):R106.

52. Robinson MD, McCarthy DJ, Smyth GK. edgeR: a Bioconductor package for differential expression analysis of digital gene expression data. Bioinformatics. 2010;26(1):139-40.

53. Huang da W, Sherman BT, Lempicki RA. Bioinformatics enrichment tools: paths toward the comprehensive functional analysis of large gene lists. Nucleic acids research. 2009;37(1):1-13.

54. Jang H, Choi DE, Kim H, Cho EJ, Youn HD. Cabin1 represses MEF2 transcriptional activity by association with a methyltransferase, SUV39H1. The journal of biological chemistry. 2007;282(15):11172-9.

55. Ying QL, Wray J, Nichols J, Batlle-Morera L, Doble B, Woodgett J, et al. The ground state of embryonic stem cell self-renewal. Nature. 2008;453(7194):519-23.

56. Handoko L, Xu H, Li G, Ngan CY, Chew E, Schnapp M, et al. CTCF-mediated functional chromatin interactome in pluripotent cells. Nature genetics. 2011;43(7):630-8.

57. Hayashi K, Ohta H, Kurimoto K, Aramaki S, Saitou M. Reconstitution of the mouse germ cell specification pathway in culture by pluripotent stem cells. Cell. 2011;146(4):519-32.

58. Rathjen J, Lake JA, Bettess MD, Washington JM, Chapman G, Rathjen PD. Formation of a primitive ectoderm like cell population, EPL cells, from ES cells in response to biologically derived factors. Journal of cell science. 1999;112 (Pt 5):601-12.

59. Zhou W, Choi M, Margineantu D, Margaretha L, Hesson J, Cavanaugh C, et al. HIF1alpha induced switch from bivalent to exclusively glycolytic metabolism during ESC-to-EpiSC/hESC transition. The EMBO journal. 2012;31(9):2103-16.

60. Kim J, Chu J, Shen X, Wang J, Orkin SH. An extended transcriptional network for pluripotency of embryonic stem cells. Cell. 2008;132(6):1049-61.

61. Kondoh H, Lleonart ME, Gil J, Wang J, Degan P, Peters G, et al. Glycolytic enzymes can modulate cellular life span. Cancer Research. 2005;65(1):177-85.

62. Esch D, Vahokoski J, Groves MR, Pogenberg V, Cojocaru V, Vom Bruch H, et al. A unique Oct4 interface is crucial for reprogramming to pluripotency. Nature cell biology. 2013;15(3):295-301.

63. Lee J, Kim HK, Han YM, Kim J. Pyruvate kinase isozyme type M2 (PKM2) interacts and cooperates with Oct-4 in regulating transcription. The international journal of biochemistry & cell biology. 2008;40(5):1043-54.

64. Wolf A, Agnihotri S, Micallef J, Mukherjee J, Sabha N, Cairns R, et al. Hexokinase 2 is a key mediator of aerobic glycolysis and promotes

tumor growth in human glioblastoma multiforme. Journal of experimental medicine. 2011;208(2):313-26.

65. Wong N, Ojo D, Yan J, Tang D. PKM2 contributes to cancer metabolism. Cancer letters. 2015;356(2 Pt A):184-91.

66. Chen Z, Zhang H, Lu W, Huang P. Role of mitochondria-associated hexokinase II in cancer cell death induced by 3-bromopyruvate. Biochimica et biophysica acta. 2009;1787(5):553-60.

67. Chen Z, Lu W, Garcia-Prieto C, Huang P. The Warburg effect and its cancer therapeutic implications. Journal of bioenergetics and biomembranes. 2007;39(3):267-74.

68. Christofk HR, Vander Heiden MG, Harris MH, Ramanathan A, Gerszten RE, Wei R, et al. The M2 splice isoform of pyruvate kinase is important for cancer metabolism and tumour growth. Nature. 2008;452(7184):230-3.

69. Patra KC, Wang Q, Bhaskar PT, Miller L, Wang Z, Wheaton W, et al. Hexokinase 2 is required for tumor initiation and maintenance and its systemic deletion is therapeutic in mouse models of cancer. Cancer cell. 2013;24(2):213-28.

70. Wong N, De Melo J, Tang D. PKM2, a Central Point of Regulation in Cancer Metabolism. International journal of cell biology. 2013;2013:242513.

ABSTRACT IN KOREAN

국문 초록

줄기세포는 특정세포로의 분화 및 유지에 있어서 epigenetic change 에 의해 cell fate determination 이 일어나고 이러한 epigenetic regulation 에 misregulation 이 일어나면 cancer 나 aging 과 같은 aberrant 한 development 가 일어나게 된다. 다른 세포들과 마찬가지로 줄기세포도 extracellular signaling 에 따라 metabolic state 를 조절하게 되는데, 이렇게 대사과정 중에 발생하는 NAD+, acetyl-CoA, α-ketoglutarate, SAM (S-adenosyl methionine)등과 같은 metabolite 나 metabolic enzyme 이 post-transcriptional modification 에 substrate 로 사용되어 histone 이나 DNA 의 modification 이 일어나게 된다. 따라서 이러한 metabolite 들의 level 변화는 chromatin modifying enzyme 에 영향을 주게 되어 epigenetic change 가 일어나게 되고, 또한 이러한 metabolic state 의 조절이 signal transduction 이나 cell hierarchy 에 영향을 준다고 알려져 있다. 특히 포도당을 에너지로 바꿔주는 첫 번째 단계에 관여하는 glycolysis related gene 들은 early embryogenesis 과정에서 highly accelerate 된다는 사실이 알려져 있다. 특히 최근 들어 줄기세포에서 이러한 high glycolytic flux 유지가 중요하다는 연구내용들이 보고되고 있다. 여러 선행 결과들을 통해 줄기세포의 전분화성 유지에 있어서

대사의 첫 단계인 해당과정이 높은 수준으로 유지되어야 한다는 사실은 확인되었지만 어떠한 factor 에 의해 높은 수준의 metabolic flux 가 유지되고, 어떠한 경로를 통해 high metabolic flux 가 줄기세포의 전분화성 유지에 관여하는지는 알려진바 없다.

본 연구에서는 metabolic flux 와 줄기세포의 전분화성간의 연관성을 찾기 위해 줄기세포의 core pluripotency factor 와 해당과정에 관여하는 대사체와의 관계에 주목하였다. 줄기세포의 core pluripotency factor 인 Oct4, Sox2, Nanog 에 의해 줄기세포의 대사과정이 조절되는지 알아보기 위해, 이들 단백질 level 의 변화에 따른 줄기세포의 metabolic flux 의 변화를 살펴보았다. 그 결과 줄기세포의 전분화성 유지에 가장 중요한 핵심인자인 Oct4 의존적으로 core pluripotency factor 의 발현과 metabolic flux 가 변하는 사실을 확인하였고, genome-wide ChIP-sequencing 을 통한 분석 결과 상당히 많은 glycolytic gene 에서 core pluripotency factor 인 Oct4, Sox2, Nanog 이 co-occupy 되어있는 것을 확인할 수 있었다. 이 중 Oct4 에 의해 직접적으로 조절되는 glycolytic enzyme 을 스크린 한 결과 hexokinase 2 (Hk2)와 pyruvate kinase M2 (Pkm2) 만이 mRNA 와 protein level 모두 Oct4 의존적으로 변한다는 사실을 확인할 수 있었다. 마지막으로 Hk2 와 Pkm2 에 의해 높은 수준의 metabolic flux 가 유지되고, 이를 통해 줄기세포의 전분화성이

유지되는지 확인하기 위해 Hk2 와 Pkm2 가 과발현 된 줄기세포를 이용한 실험들을 진행하였다. 그 결과 다양한 분화 조건에서도 Hk2 와 Pkm2 의 과발현을 통해 높은 수준의 metabolic flux 가 유지되고 줄기세포의 전분화성이 유지되며 분화가 지연된다는 새로운 사실을 확인하였다.

주요어 : 줄기세포, core pluripotency factors, Oct4, 대사작용, 해당과정, hexokinase 2 (Hk2), pyruvate kinase M2 (Pkm2), 전분화성, 분화

학 번 : 2009-30601